Title

The discovery of a catalytic RNA within RNase P and its legacy.

Journal

Journal of Biological Chemistry, 300(6)

Authors

Kirsebom, Leif

Liu, Fenyong

McClain, William

Publication Date

2024-06-01

DOI

10.1016/j.jbc.2024.107318

Peer reviewed

The discovery of a catalytic RNA within RNase P and its legacy

Received for publication, September 18, 2023, and in revised form, April 12, 2024 Published, Papers in Press, April 25, 2024,
https://doi.org/10.1016/j.jbc.2024.107318

Leif A. Kirsebom[1,*], **Fenyong Liu**[2,*], **and William H. McClain**[3,*]

From the [1]*Department of Cell and Molecular Biology, Uppsala University, Uppsala, Sweden;* [2]*School of Public Health, University of California, Berkeley, California, USA;* [3]*Department of Bacteriology, University of Wisconsin-Madison, Madison, Wisconsin, USA*

Reviewed by members of the JBC Editorial Board. Edited by Karin Musier-Forsyth

Sidney Altman's discovery of the processing of one RNA by another RNA that acts like an enzyme was revolutionary in biology and the basis for his sharing the 1989 Nobel Prize in Chemistry with Thomas Cech. These breakthrough findings support the key role of RNA in molecular evolution, where replicating RNAs (and similar chemical derivatives) either with or without peptides functioned in protocells during the early stages of life on Earth, an era referred to as the RNA world. Here, we cover the historical background highlighting the work of Altman and his colleagues and the subsequent efforts of other researchers to understand the biological function of RNase P and its catalytic RNA subunit and to employ it as a tool to downregulate gene expression. We primarily discuss bacterial RNase P–related studies but acknowledge that many groups have significantly contributed to our understanding of archaeal and eukaryotic RNase P, as reviewed in this special issue and elsewhere.

Francis Crick's note to the RNA Tie Club titled "On degenerate templates and the adaptor hypothesis" introduced the existence of an adaptor molecule that connects the gene sequence with the protein sequence [(http://resource.nlm.nih.gov/101584582X73) (1); the informal scientific RNA Tie Club was founded 1954 for scientists with an interest in protein synthesis and the genetic code (2)]. A few years later, a small adaptor molecule (about 75 nt, in length) termed pH 5 RNA or soluble RNA was identified biochemically. The molecule's sedimentation coefficient was determined to be 4S, and in 1960, it was renamed tRNA (3–5). Subsequently, sequencing of a yeast alanine tRNA revealed a 76 residue-long polynucleotide chain (6).

To pursue the understanding of tRNA structure and function, Sidney Altman began his postdoctoral work under the mentorship of Sydney Brenner and Francis Crick at the Medical Research Council Laboratory of Molecular Biology (LMB) in Cambridge, England. John Smith was recruited to the LMB for his expertise in the primary structure determinations of RNAs, and he headed the new RNA biochemistry subsection under Brenner and Crick. Two of Altman's postdoctoral colleagues were Bill McClain and Hugh Robertson, who brought expertise in bacteriophage genetics and ribonuclease purification, respectively. The amber UAG triplet is nonsense in mRNA (*i.e.*, does not correspond to an amino acid codon) and terminates protein synthesis in normal cells. However, the amber UAG triplet is translated in a cell having a nonsense suppressor tRNA that inserts a specific amino acid, for example, tyrosine ($tRNA^{Tyr}Su3$). Brenner and his laboratory developed the tactics for applying genetic selections, first by providing an active amber-suppressor $tRNA^{Tyr}Su3$ gene carried by bacteriophage φ80 and then by isolating derivative strains with diminished suppressor tRNA activity or with an altered amino acid acceptor specificity. The first phase established that suppression resulted from a nucleotide change in the tRNA anticodon (7). At the project's outset, the notion was that a mutated tRNA would exhibit diminished function and appear as a less active suppressor tRNA when assayed (8). Using a polyacrylamide gel–based analysis of *in vivo* ^{32}P-labeled RNAs, Altman reported the absence of mutant $tRNA^{Tyr}Su3$ and the presence of a new RNA that was susceptible to cellular degradation and migrated more slowly in gels than "WT" $tRNA^{Tyr}Su3$ (9).

To Altman's (and science's) lasting benefit, base-change mutations in tRNA perturbed molecular folding and thus the kinetics with which RNA-processing enzymes handle mutant tRNA precursor intermediates. Consequently, these intermediates accumulate, spending more time in incomplete maturation states. Upon subjecting this new RNA species to ribonuclease T_1 digestion, Altman *et al.* estimated that it contains "approximately forty more nt than the usual tyrosine tRNA". RNA sequence determination confirmed the molecule as a $tRNA^{Tyr}Su3$ precursor with a 5′-pppG remaining from transcription initiation and containing 41 extra nt in the 5′ precursor segment plus three additional nt in the 3' segment of the mature $tRNA^{Tyr}Su3$ [Fig. 1*A* (10); it was later shown that the 5′ leader is 43 nt long]. The precursor did not contain modifications. The detection of a nucleolytic activity (later named RNase P) in the extracts of *Escherichia coli* producing $tRNA^{Tyr}Su3$ from its precursor RNA announced the entry of RNase P into the biogenesis of mature tRNAs. The large "Altman RNA molecule" represented the first sequence of a tRNA precursor and reflected the general nature of and structure of tRNA precursor transcripts. Previous work had reported on large unstable transcripts in eukaryotes, possibly tRNA precursors, but these molecules were not sequenced (11–13). In conclusion, the combined results indicated that tRNA genes in both bacteria and mammals are transcribed as

* For correspondence: Leif A. Kirsebom, leif.kirsebom@icm.uu.se; Fenyong Liu, liu_fy@berkeley.edu; William H. McClain, wmcclain@wisc.edu.

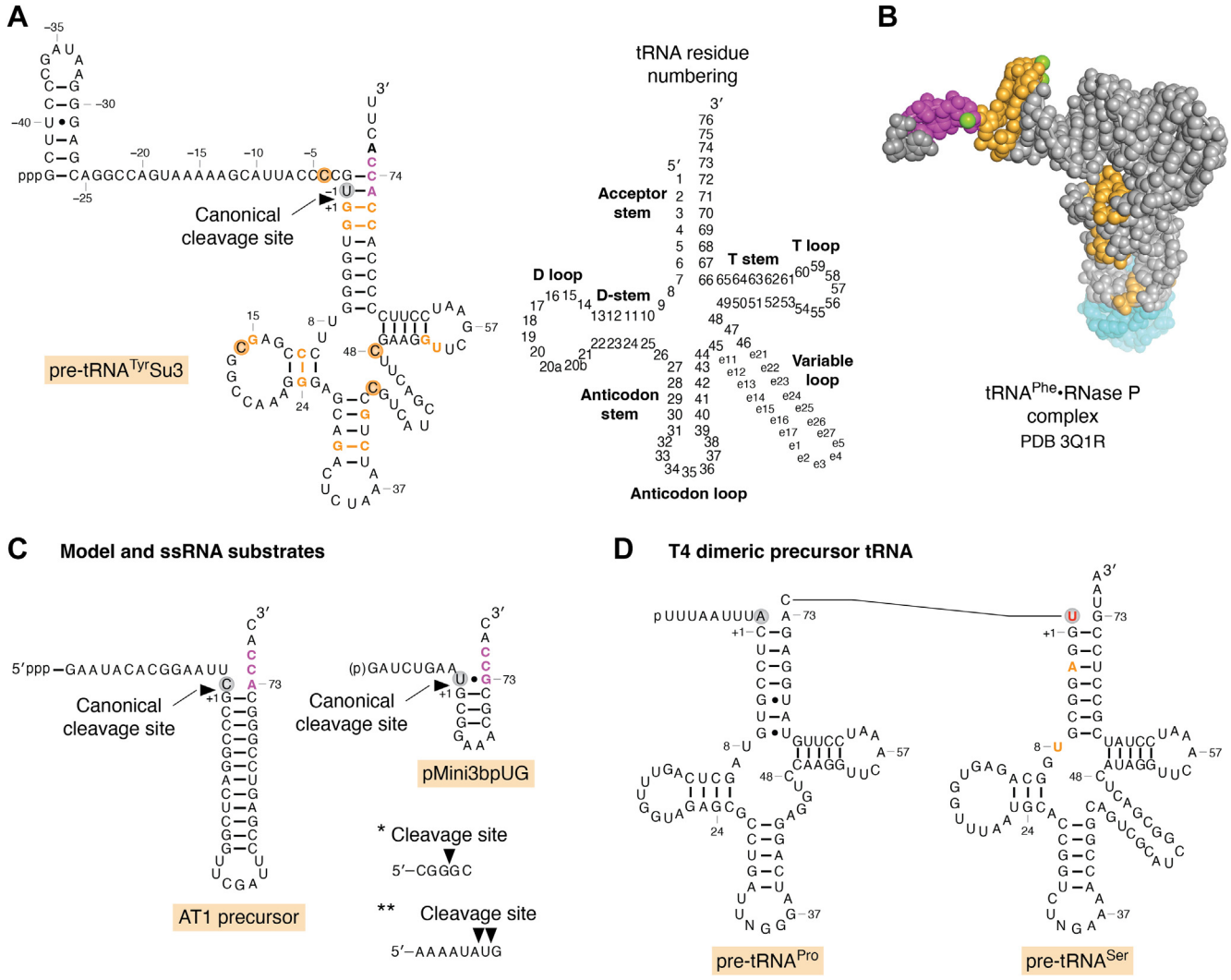

Figure 1. Structures of monomeric, dimeric, and model RNase P substrates. *A*, residues in pre-tRNA^{Tyr}Su3 implicated or demonstrated to be important in RNase P processing *in vivo* and/or *in vitro* are marked in *orange* and *magenta* (residues at the 3′ end that bp with the 5′GGU sequence in the RPR forming the "RCCA-RPR interaction"; Fig. 2*C*), while U_{-1} is highlighted with a *gray* circle. With respect to changes in pre-tRNA^{Tyr}Su3 at the positions marked in *orange* and *magenta*, see the main text for details (9, 20, 44, 45, 85, 86, 269). Numbering of tRNA residues according to Steinberg *et al.* (270). *B*, the crystal structure of matured tRNA^{Phe} bound to RNase P [pdb 3Q1R (33)]. The color code for some pre-tRNA^{Su3}Tyr residues (in *orange*, G_{+1}, G_{+2}, U_{+8}, C_{+11}, G_{+15}, G_{+24}, G_{+30}, C_{+40}, C_{+71}, and C_{+72}; in *magenta*, A_{+73}, C_{+74}, and C_{+75}) shown to affect RNase P cleavage is the same as in panel A except U_{+8}, but see panel E, T4 tRNA^{Ser}. The *green spheres* represent Me(II)-ions seen in the RNase P-tRNA crystal structure. The *turquoise spheres* correspond to extra residues (not originally present in tRNA), which were added to promote crystallization (33). *C*, structures of model and ssRNA substrates. i) The AT1 precursor is derived by "combining" the acceptor-stem, the T-stem, and the T-loop of *Escherichia coli* tRNA^{Phe} (64), and the pMini3bpUG is derived from the *E. coli* pre-tRNA^{Ser}Su1 precursor (98). Residues marked in *magenta* in both substrates interact with the 5′ GGU in the RPR, while C_{-1} and U_{-1} are highlighted with *gray* circles. The two short ssRNA substrates are cleaved by **Bsu* RNase P (holoenzyme) and *Bsu* RPR/*Eco* C5 protein [reconstituted holoenzyme (70)] and ***Bsu* RNase P [holoenzyme (69)]. The cleavage sites are marked with *solid arrows*. *D*, the dimeric T4 Pro-Ser tRNA precursor. Residues influencing RNase P processing *in vivo* and *in vitro*, A_{+2} and U_{+8}, are marked in *orange* (21). The *red*-colored U corresponds to pre-tRNA^{Ser} U_{-1}.

longer precursor RNAs, pre-tRNAs, which are enzymatically converted into mature tRNAs. Evidence soon emerged for parallels even with phage-encoded tRNAs.

McClain's interest in RNA sequencing led him to focus on the small RNAs of bacteriophage T4 that turned out to be tRNAs. Finding two RNAs with sizes longer than those expected of tRNAs seemed outside his interest. However, Robertson suggested incubating the longer-sized RNAs with his "30,000*g* supernatant fraction of *E. coli* MRE600 …," which contained RNase P but was otherwise relatively free of RNases. The incubation of one of the large T4 RNAs produced two smaller RNA products (later identified as tRNA^{Pro} and tRNA^{Ser}, each with a 5′ end of the corresponding mature tRNA), while the second produced two smaller RNA products, tRNA^{Thr} and tRNA^{Ile} (14). Altman and Smith (10) had shown that the same extract also cleaved the precursor tRNA^{Tyr}Su3 to generate mature tRNA^{Tyr}Su3. Because neither of the larger T4 bands contained a 5′-pppG, neither is a primary transcript. Thus, these analyses concluded that a tRNA precursor could have the sequences of two tandem tRNAs, then a novelty in tRNA biology. The processing of these pre-tRNAs were later shown to depend on the *E. coli* host enzymes, BN nuclease, tRNA nucleotidyltransferase, and RNase P, to generate tRNAs with matured 5′ and 3′ termini (15, 16).

An endoribonuclease from the *E. coli* 30,000*g* supernatant fraction (see above) was purified and demonstrated to be responsible for removing the 5′ leader (Fig. 1*A*), and the ribonuclease was named RNase P (17). At the same time, temperature-sensitive (*ts*) *E. coli* mutants defective in generating functional $tRNA^{Tyr}Su3$ nonsense suppressors were isolated by Schedl and Primakoff and by Shimura and Ozeki (18, 19). Genetic mapping identified at least two genes associated with RNase P activity, and these genes were later shown to encode for the RNase P protein (in *E. coli*, the subunit is called C5 protein; see below) and the other M1 RNA [for reviews of the early works (20, 21)].

The Altman laboratory continued the work on RNase P and discovered that M1 RNA is essential for *E. coli* RNase P activity. In 1981, Kole and Altman stated, "The absence of any demonstrable hydrolytic activity of the C5 protein is striking and implies that the M1 RNA must be involved in activating the catalytic mechanism of the RNase P complex" (22). The subsequent reconstitution of RNase P activity with purified M1 RNA and C5 protein allowed this conclusion: "The catalytic activity resides in M1 RNA." (23). Guerrier-Takada and Altman conclusively showed that this is indeed the case using M1 RNA produced by *in vitro* SP6 RNA polymerase transcription (24). With pure RNA in hand, the Altman laboratory continued to experimentally tackle the radical concept that an RNA, the M1 RNA, acts as a true trans-acting multiple-turnover catalyst that follows Michaelis–Menten kinetics with substrate binding, cleavage, and product release. For activity, RNase P requires Mg^{2+}, and in the RNA-alone reaction, a higher Mg^{2+} concentration was needed than in the presence of the C5 protein (23–25). All of the scientific community did not embrace the discovery of M1 RNA as a bona fide catalyst. At about the same time, however, Cech et al. were identifying and characterizing a self-splicing RNA, the group I intron. The Cech group coined the term ribozyme to distinguish RNA catalysts from protein enzymes (26). Whereas the group I intron RNA acted in *cis* within the same RNA molecules, M1 RNA is a *trans*-acting ribozyme allowing multiple turnover.

Understanding of an RNA catalyst: Making sense of the unexpected

The breakthrough discoveries that RNA can act as a catalyst inspired increased research in RNA biology [and the "RNA world" (27, 28)], including RNase P. Several laboratories and research groups pursued efforts to unravel the function of RNase P and its subunits by studying bacterial, archaeal, and eukaryotic RNase P. In contrast to bacterial RNase P, archaeal and eukaryotic RNase P are composed of 4 to 5 and 9 to 10 proteins, respectively, and one RNA (29). Despite these differences in protein composition, the RNA has been demonstrated to be the catalytic subunit in all domains of life (30–32). The crystal and cryo-EM structures of bacterial, archaeal, and eukaryotic RNase P in complex with tRNA or pre-tRNA have been reported (33–37) and advanced our understanding of this catalytic RNA.

Here, we focus on bacterial RNase P and survey findings that have contributed to our current understanding of the function of RNase P and its subunits by discussing the following: (i) pre-tRNA recognition and cleavage site selection by RNase P, (ii) RNase P RNA regions that interact with the substrate and the RNase P protein, (iii) importance of residues and chemical groups at and near the RNase P cleavage site, (iv) metal(II)-ions and the current understanding of the cleavage mechanism, and (v) some future challenges. Following this, we will discuss the use of RNase P and its catalytic RNA as pharmaceutical and biotechnology tools. We refer to RNase P RNA as RPR and the protein subunit as RPP (in *E. coli* or *Eco*, they are referred to as M1 RNA and the C5 protein, respectively). Residues in the pre-tRNA 5′ leader are referred as N_{-1}, N_{-2} etc, where N_{-1} corresponds to the residue immediately 5′ of the scissile phosphate (Fig. 1). We refer to recent reviews for discussions of archaeal and eukaryotic RNase P (38–42).

RNase P and its substrates: Recognition and versatility

To understand how RNase P recognizes and interacts with pre-tRNA, Altman took advantage of available $tRNA^{Tyr}Su3$ mutants (Fig. 1) coded by bacteriophage Φ80. These were used at the LMB to study and understand tRNA structure and function (7). Early on, it was realized that changes either in the tRNA body or in the 5′ leader influenced the level of mature tRNA *in vivo*. For example, changing residue G15 to A in the $tRNA^{Tyr}Su3$ precursor (pSu3A15) alters the structure such that pSu3A15 accumulates *in vivo*, and it is processed less efficiently by RNase P *in vitro* [Fig. 1*A* (7, 9, 43–46)]. Moreover, disrupting a base-paired stem structure in pre-tRNAs resulted in less efficient RNase P cleavage *in vitro*. Introducing second-site mutations that restored the base-pairing (or the tertiary structure) improved RNase P cleavage and increased the yield of matured tRNA *in vivo*. McClain *et al.* subsequently identified pre-tRNAs transcribed from the bacteriophage T4 genome [see above (14, 47)], which carries eight tRNA genes, and six of these were identified as dimeric precursor-tRNAs (48, 49). For some of these precursor variants, disruption of the tRNA structure influenced the amount of tRNA produced relative to the WT tRNA as did the absence of the 3′ CCA (16, 50–52). Together, these studies suggested that RNase P recognizes the tRNA domain of a pre-tRNA (Fig. 1, *A* and *B*). This conclusion was later corroborated *in vitro* by several research groups using different approaches such as genetics, chemical footprinting, and nucleotide analog interference mapping (NAIM) and ultimately when the RNase P-tRNA crystal structure was obtained (33, 53–55); see below.

RNase P cleavage results in tRNAs having seven bp in the acceptor stems; however, $tRNA^{His}$ and $tRNA^{SeCys}$ are exceptions (56–59) as they have 8 bp acceptor-stems. In eukaryotes, RNase P cleavage of the $tRNA^{His}$ precursor results in a seven bp-long acceptor-stem, and a guanylyltransferase adds the extra G at the 5′ end to form 8 bp with a single-stranded 3′-CCA end (60). Together, these data emphasized that the tRNA acceptor-stem is an important determinant for RNase P recognition and cleavage.

The importance of the acceptor-stem for RNase P catalysis was further corroborated using chimeric pre-tRNAs where the $tRNA^{His}$ acceptor-stem was introduced into pre-$tRNA^{Tyr}$Su3 and yeast pre-$tRNA^{Ser}$ (61, 62). Experiments by Green and Vold (63) also emphasized the importance of the tRNA acceptor-stem in the processing of a multimeric tRNA precursor (carrying six complete and one incomplete tRNA sequence) *in vitro* by *Bacillus subtilis* (*Bsu*) RPR without the protein component. In collaboration with the Altman laboratory, McClain showed that *Eco* RPR, both with and without the *Eco* RPP, cleaved synthetic model hairpin-loop substrates efficiently at the canonical cleavage site [Fig. 1*C* (64)]. These model substrates represented the tRNA acceptor-stem, T-stem, and the T-loop that forms a well-defined domain in the crystal structure of tRNA (64–66). This finding is consistent with the importance of the tRNA acceptor-stem in cleavage by RNase P and led to the development of the external guide sequence technology in the Altman laboratory (discussed further below).

Following an *in vitro* evolution protocol, substrates were selected that were processed by *Eco* RPR, with and without *Eco* RPP. Processing of these substrates by *Eco* RPR in the absence and presence of *Eco* RPP agreed with earlier work that the acceptor-stem plays an essential role in the *Eco* RNase P–catalyzed reaction (67). Furthermore, *in vitro* evolution using *Bsu* RPR identified two substrate classes (I and II). Class I carries a stem-loop mimicking the tRNA T-stem/loop (TSL) motif, a single-stranded region in place of the acceptor-stem and a 3′ CCA motif. The class II members have seven base-pairs-long helices appended to either 3′ trailers or to a loop structure. Both these substrate types were cleaved by *Bsu* RPR 5′ of a G residue, in the single stranded region (class I) and in the stem structure (class II). Relative to cleavage of a pre-$tRNA^{Phe}$ substrate, *Bsu* RPR cleaved these variants with less efficiency. Comparing cleavage by *Bsu* RPR and *Eco* RPR showed that cleavage efficiency was lower using *Eco* RPR. The difference was attributed to structural differences between *Eco* RPR and *Bsu* RPR [Fig. 2, *A* and *B*; for details see (68)]. Later, it was demonstrated that both *Eco*- and *Bsu*-reconstituted holoenzymes (RPR assembled with the RPP) cleave short ss RNAs (≥5 residues long) albeit with several orders of magnitudes of lower efficiencies relative to cleavage of pre-tRNAs. As for the *in vitro*–selected substrates, the ssRNAs were cleaved 5′ of guanosines [Fig. 1*C* (69, 70)]. These data are consistent with *Eco* RPR cleaving 5′ of guanosines in single-stranded regions of pre-tRNAs having shortened acceptor-stems with and without RPP (71); these results led to the suggestion that a guanosine at the cleavage site functions as a guiding nucleotide (71, 72). Cleavage of ssRNAs and *Bsu* RPR having 5′ and 3′ extensions by *Bsu* RNase P led to the suggestion that in *B. subtilis* cells, the RNase P is involved in autolytic processing of the RPR transcript (69). In *E. coli*, the processing of the 3′ end of the RPR precursor involves the endoribonuclease E (73, 74).

Together with the finding that RNase P also processes other RNAs (see below), these data uncovered the versatility of RNase P function with respect to substrate recognition and processing. Notably, the demonstration that *Eco* RPR can cleave pre-tRNAs at alternative sites, in particular without the RPP, paved the way to identify key residues in RPR (and in its substrate) playing a role in recognition of the correct cleavage site and to identify the function of the RPP. Moreover, it was clear that *Eco* RPR—with and without the RPP—cleaves model hairpin-loop substrates (64). This result, together with advances in RNA chemical synthesis (75), established the basis for the design and study of cleavage of substrates carrying unnatural nucleobases at selected positions. Several research groups have used this strategy [*e.g.*, (76)].

Bacterial RPR: The S-domain and induced fit

On the basis of the secondary structures, bacterial RPR can be divided into three different types: A (Ancestral type; *e.g.*, *E. coli* RPR), B (Bacillus type), and C [*e.g.*, *Thermomicrobium roseum*, member of the phylum *Chloroflexi* (41)]. Here, we focus on the functions of the different regions and domains in bacterial type A and type B RPR (Fig. 2, *A* and *B*).

Deletion of *Eco* RPR regions resulted in either loss of activity or catalytically active fragments but with altered substrate specificities. Mixing certain inactive RPR fragments (with nonoverlapping deletions) produced active complexes. Interestingly, deleting residues 94 to 204 of the *Eco* RPR S-domain (Fig. 2*A*) abolishes cleavage of pre-$tRNA^{Tyr}$Su3 (with and without *Eco* RPP), albeit this variant (Δ94–204) still cleaves *Eco* pre-4.5S RNA (a natural RNase P substrate, see below) in the presence of *Eco* RPP (77, 78). Subsequently, Pan suggested that *Bsu* RPR can be divided into two structural domains; the specificity (S-) and catalytic (C-) domains. While neither of these two domains were catalytically active alone, activity was restored when they were mixed together [Fig. 2, *A* and *B* (79)]. Collectively, the data show the importance of the RPR domains irrespective of RPR type. The data also suggest that binding and cleavage of pre-4.5S RNA, unlike pre-tRNA, do not require an intact S-domain for processing by *Eco* RNase P (77, 78). However, it was subsequently demonstrated that bacterial types A and B RPR C-domains lacking the S-domain are catalytically active, with and without the RPP, even with pre-tRNAs as substrates although pre-tRNA binds the C-domain with less affinity (80–84).

Before the RNase P-tRNA crystal structure was resolved, cross-linking, modification interference, and genetic and biochemical data suggested that particular residues and chemical groups in the pre-tRNA TSL region interact with the RPR S-domain (both type A and B) (82, 85–92). Specifically, it was suggested that 2′-OH groups in the T-loop/stem at positions 54, 56, 61, and 62 (see Fig. 1, *A* and *B*) influence binding of pre-tRNA to the type B *Bsu* RPR (91, 93). In addition, the exocyclic amine at position 4 of C_{56} was postulated to interact with the RPR. These chemical groups were suggested to interact with residues in the P11 region in the S-domain (Fig. 2). In particular, the data indicated that the 2′-OH at position 62 interacts with A_{230} of *Bsu* RPR (corresponding to A_{233} in *Eco* RPR; Fig. 2, *A* and *B*). Other RPR residues in the

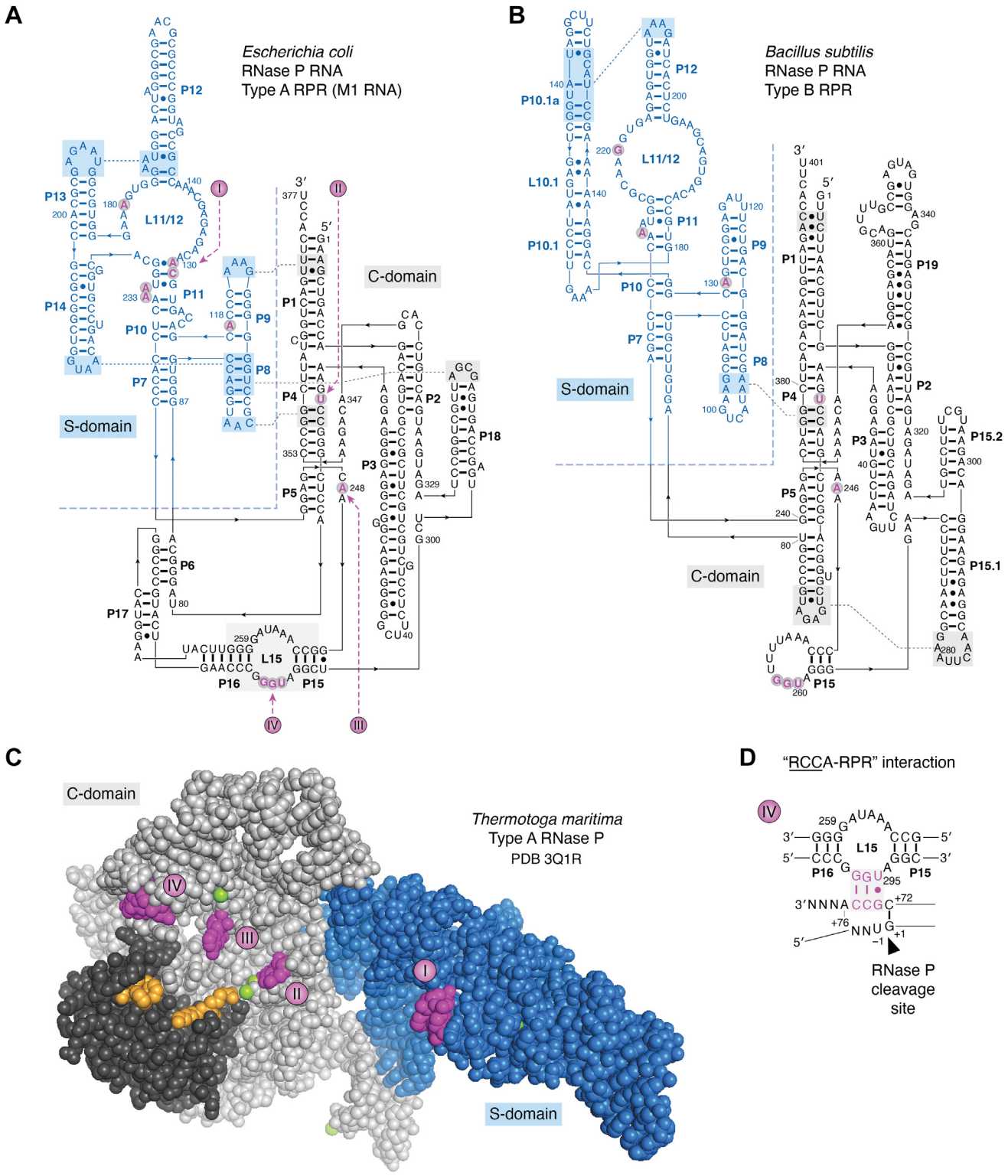

Figure 2. Structures of the bacterial RNase P RNA and RRP. *A*, the predicted secondary structure of the type A *Eco* RPR (271, 272). The border separating the S- and C-domains is marked with the *dotted line*. Residues highlighted in *magenta* correspond to functionally important residues discussed in the main text, see also Fig. 2*B*: I, residues C_{128}, A_{129}, A_{232} and A_{233}, which are part TSB (the T-loop-stem binding site); II, residue U_{69}, which interact with the tRNA acceptor-stem (the "U_{69}-amino acid stem interaction") and is involved in coordinating Mg^{2+}; III, residue A_{248}, which stacks on top of the tRNA G_{+1}/C_{+72} pair and is positioned near N_{-1} in the substrate forming the "A_{248}/N_{-1}" interaction; and IV, residues G_{292}, G_{293}, and U_{294} which pairs with $D_{+73}C_{+74}$ and C_{+75} in the substrate forming the "RCCA-RPR" interaction (highlighted in panel C), D refers to the tRNA discriminator base. The residue C_{92} marked in *orange* is positioned close to C_{-3} in pre-tRNA^{Tyr}Su3 as determined by UV-crosslinking (99). For references, see the main text. *B*, the predicted secondary structure of the type B *Bsu* RPR (271, 272). The border separating the S- and C-domains is marked with the *dotted line*. Residues highlighted in *magenta* correspond to residues U_{51}, A_{130}, G_{220}, A_{230}, and G_{258}-U_{260} [part of the "RCCA-RPR" interaction in type B RPR (116)] discussed in the main text (see above). *C*, the crystal structure of type A RNase P, RPP, from *Thermotoga maritima* (RPR C-domain, *light gray*; RPR S-domain, *blue*; RPP, *dark gray*). Residues marked in *magenta* are mapped on *Eco* RPR in panel A as indicted (spheres in *magenta*, marked I–IV, correspond to the spheres in Fig. 2*A*). The RPP amino acids marked in *orange*

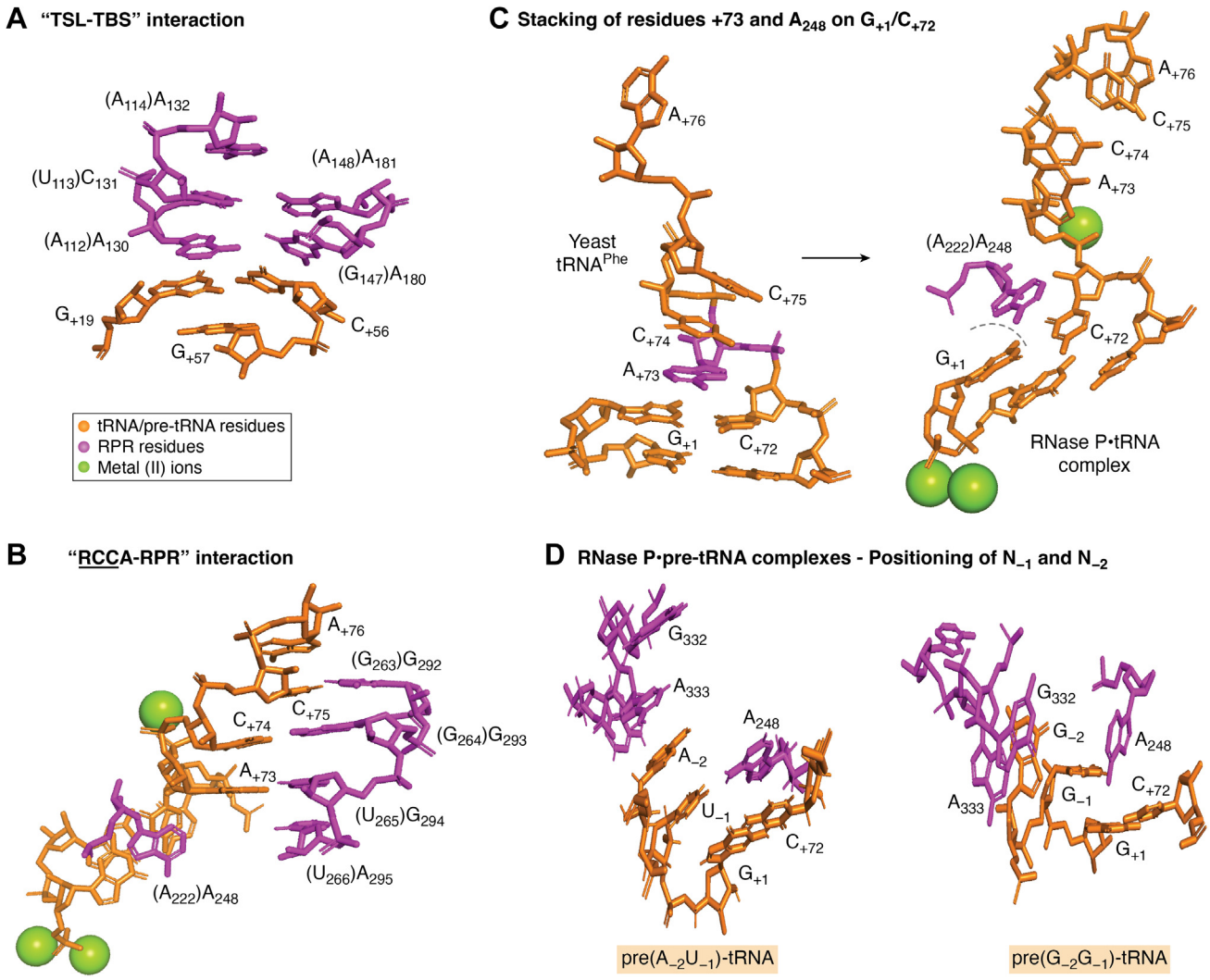

Figure 3. Stacking interactions and base pairing between bacterial type A RPR and tRNA/pre-tRNA. tRNA/pre-tRNA residues are colored in *orange* and RPR residues in *magenta*. The numbering corresponds to *Eco* RPR (see Fig. 2*A*) while residues in parenthesis refers to the *Thermotoga maritima* RPR numbering in the RNase P-tRNA crystal structure. *A*, stacking between the tRNA TSL-region and residues in the TBS in the S-domain as observed in the RNase P-tRNA structure. *B*, the "RCCA-RPR" interaction in the RNase P-tRNA structure, see also Fig. 2*D*. The *green spheres* represent metal(II) ions. *C*, *left* panel, stacking of the discriminator base (A_{+73}, colored in *magenta*) on the yeast $tRNA^{Phe}$ G_{+1}/C_{+72}. *Right* panel, stacking of A_{248} (*Eco* RPR numbering) on the tRNA G_{+1}/C_{+72} pair in the RNase P-tRNA structure. The *green spheres* represent metal(II) ions. *D*, interactions between N_{-1}/N_{-2} in the pre-tRNA 5′ leader and *Eco* RPR in the cryo-EM RNase P-pre($A_{-2}U_{-1}$)-tRNA (*left* panel) and RNase P-pre($G_{-2}G_{-1}$)-tRNA (*right* panel) structures. For *Eco* RPR residues numbering, see. 2A. The images were created using PyMOL (Schrödinger, LLC), PDB 1EHZ [yeast $tRNA^{Phe}$ (273)], PDB 3Q1R (33), PDB 7UO1 [cryo-EM, RNase P-pre($A_{-2}U_{-1}$)-tRNA (37)], and PDB 7UO0 [cryo-EM, RNase P-pre($A_{-2}U_{-1}$)-tRNA (37)]. TSL, T-stem loop.

S-domain suggested to contact the TSL region were A_{130} and G_{220} (in *Bsu* RPR), corresponding to A_{118} and A_{180} in *Eco* RPR [Fig. 2, *A* and *B* (91, 93, 94)]. The bacterial RNase P-tRNA crystal structure (33) later revealed that base stacking is a main contributor to the interaction between TSL (the "tRNA elbow") and the RPR. The RPR "base stacking" platform motif is formed by two intertwined T-loops (95), which include residues A_{130}/C_{131} and A_{180}/A_{181} [*Eco* RPR numbering; Figures 2*A* and 3*A* ((95), see also (96))]. The TSL-binding site is referred to as TBS, and the interaction is referred as the TSL–TBS interaction.

Assays using pre-$tRNA^{Phe}$ variants with 2′-OH changed to 2′-H substitutions at specific positions in the TSL region and at the cleavage site revealed reduced cleavage by *Bsu* RPR compared to the unmodified substrate (91). It was inferred that catalysis is dictated also by interactions distal to the cleavage site. A conformational change/spatial rearrangement upon *Bsu* RPR–pre-tRNA complex formation was postulated to depend on the TSL–TBS interaction (82). Furthermore, *Eco* RPR cleaves model hairpin-loop precursors based on the acceptor-stem, T-stem, and T-loop of the *E. coli* pre-$tRNA^{Ser}$Su1; this cleavage occurs preferentially at the correct site with and

interact with a pre-tRNA 5′ leader that was soaked into the crystal. The *green spheres* correspond to metal(II)-ions located near the tRNA G_{+1}/C_{+72} and U_{69} in the RPR. The image was created using PyMOL (Schrödinger, LLC) and PDB 3Q1R, although the tRNA was omitted for clarity (33). *D*, illustration of the "RCCA-RPR" interaction (see also Fig. 3*C*). Interacting residues marked in *magenta* and the *arrow* marks the RNase P cleavage site.

without the *Eco* RPP [see *e.g.* (97)]. Replacing the "T-loop" with tetra-loop variants reduces cleavage efficiency and shifts the cleavage site such that cleavage by *Eco* RPR occurred between N_{-2} and N_{-1} in the 5′ leader: correct cleavage occurs 3′ of N_{-1}, between N_{-1} and N_{+1} (Fig. 1). Interfering with the TBS structural topology (by mutating G_{125} and/or C_{235} in the P11-region; Fig. 2*A*) restored cleavage efficiency at the correct site leading to the suggestion that efficient and correct cleavage depends on a productive TSL–TBS interaction. These and other data provided evidence for an induced-fit mechanism for bacterial RPR-mediated cleavage [(98) see also (99)]. We also note that NAIM data suggest overlapping but not identical binding modes for pre-tRNA and mature tRNA using *Eco* RPR. Strong interference was detected at positions G_{19}, G_{53}, A_{58}, and G_{71} [Fig. 1 ((100), see also (101))]. Notably, Bothwell *et al.* (102) postulated that RNase P interacts with T-loop of the pre-tRNA and uses a measuring device to identify the cleavage site [see also (89, 103, 104)]. The "Bothwell postulate" (102) also agrees with the discussion above and that the distance between the T-loop and the tRNA 5′ terminus corresponds to the conserved 12 bp in tRNAs (Fig. 1, *A* and *B*).

In keeping with the induced-fit theory (105), a productive TSL–TBS interaction (see above) is suggested to induce a conformational change in the RPR–substrate complex, in particular at the cleavage site thereby affecting site selection and cleavage rate (98). Details of this signaling at the structural level are at present not known; however, analysis of interactions that connect the S- and C-domains might be informative (33, 106–108). Neither interfering with the P8/P18 contact, which is important for the connection between the S- and C-domains [Fig. 2*A* (33, 109, 110)], nor deleting P18 (ΔP18-variant) changed the cleavage site as assessed using a model substrate; however, the cleavage efficiency was significantly reduced in these mutants (84). The cleavage rate (k_{obs}) for the ΔP18-variant was >3000-fold lower relative to WT *Eco* RPR; the K_D for substrate binding was unchanged [see also (106–108)]. Also, the data obtained using a substrate carrying a 2′-NH_2 at N_{-1} suggested that interference with the P8–P18 interaction, the structure near the TBS, or deleting the S-domain influenced the charge distribution at the cleavage site (84). Protonation of the 2′-NH_2 (at N_{-1}) at lower pH produces a positive charge at the cleavage site resulting in a lower cleavage frequency at the correct site. At higher pH, cleavage at the correct site increases, reflecting the deprotonation of this 2′-NH_3^+. The positively charged 2′-NH_3^+ would interfere with Mg^{2+} binding at and in the vicinity of the cleavage site [see below and (111, 112)]. Together, these data suggest a role for the P8–P18(L18) interaction and P18 with respect to a productive TSL–TBS interaction (Fig. 2*A*) and the structural architecture at (and near) the cleavage site that ensures correct and efficient cleavage.

Bacterial RPR and the "RCCA–RPR" interaction

Many tRNA genes in bacteria contain the universally conserved 3′ CCA motif (113). Early studies indicated that the 3′ CCA motif of tRNA precursors affected RNase P cleavage [see above (16, 43, 50, 51)]. By studying the choice of cleavage site, it was later revealed that the 5′ GGU motif in the P15 loop in *Eco* RPR (Fig. 2) base pairs with the 3′ "RCCA-motif" [interacting residues underlined and R corresponds to the tRNA discriminator base at position 73 (114), Fig. 1, *A–C*]. This pairing is referred to as the "RCCA–RPR" interaction. It is present both with and without *Eco* RPP (115, 116) and is supported by footprinting as well as single-turnover kinetic data (94, 117, 118). The interaction is also observed in type B RPR substrate complexes (116, 119), and it is essential for catalysis in *E. coli* and *B. subtilis* cells (119, 120). The RNase P-tRNA crystal structure confirmed the "RCCA–RPR" interaction (33).

The "RCCA–RPR" interaction was suggested to anchor the substrate to the RPR, expose the cleavage site, and result in re-coordination of Mg^{2+} at and in the vicinity of the cleavage site to ensure accurate and efficient cleavage [(115); see also below]. This idea is consistent with the finding that small RNAs representing the *Eco* RPR P15 loop (Fig. 2*A*) and P15-P15.1 of type B RPR (Fig. 2*B*) mediate cleavage of both pre-tRNA and a model hairpin loop substrate each at the correct site, but with reduced efficiency (121). This observation, together with the finding that the group II intron domain V (as part of small RNAs) catalyzes hydrolysis of the exon-intron junction in trans (122), provided evidence that complex RNAs like the RPR and rRNAs are composed of functional domains (123).

Bacterial RNase P: Importance of the RPP/C5 protein and the 5′ leader

The number of protein subunits varies in RNase P: one in bacteria (RPP), four to five in archaea, and nine to ten in eukaryotes (53). As discussed above, the isolation of temperature-sensitive (*ts*) *E. coli* strains carrying mutations in the C5/RPP protein gene, *rnpA*, suggested that the *Eco* RPP is essential for activity *in vivo* (18, 19, 124, 125). Sequencing later confirmed that these *E. coli* strains indeed carry changes in *rnpA*, $C5^{A49}$ (R46H), and $C5^{ts241}$ (E71K) (45). Several overexpression protocols were tested to generate significant amounts of the *E. coli* C5 (and $C5^{A49}$) protein; the Altman laboratory developed protocols using the T7 RNA polymerase–based protein overexpression system [(126, 127); see also (128)]. This work led to the demonstration of the 1:1 stoichiometry (of the RPP and RPR) in the RNase P holoenzyme, determination of the dissociation constant for the interaction between *Eco* RPR and *Eco* RPP, and mapping of regions in *Eco* RPR that interact with *Eco* RPP (78, 126, 129). Reconstitution experiments further suggested that the *ts*-phenotype associated with $C5^{A49}$ is caused by a defect in the assembly of the RNase P holoenzyme (130). This conclusion agrees with the observation in several laboratories that the *E. coli* A49 *ts*-phenotype can be rescued by increasing the levels of RPR *in vivo*. Later findings showed that overexpressing other *Eco* RPP mutant proteins also rescues the A49 *ts*-phenotype and provided models of RPR in complex with RPP. Interestingly, single amino acid substitutions in the RPP alter substrate specificity of the reconstituted RNase P

holoenzyme (131). Experiments using RPR with deletions or single nucleotide mutations indicated that the RPR tertiary structure is a determinant for RPP recognition. Moreover, based on footprinting techniques, RPP-RNA contact sites in *Eco* RNase P were identified, and these data were used to generate structural models of the bacterial RNase P holoenzyme (132–134). Understanding RPR–RPP interactions in RNase P (type A) became possible with the availability of the crystal structure of the RNase P-tRNA complex (Fig. 2*C*). The RNase P-tRNA crystal structure and models of the complex are in good agreement (33, 133, 134).

The RPP lowers the Mg^{2+} requirement and increases cleavage efficiency *in vitro*, and it was suggested that the RPP acts as an electrostatic shield (23, 59). Subsequent studies showed that the RPP stabilizes the catalytic active RPR conformation (135, 136), modulates substrate specificity (53, 137–139), and affects the metabolic stability of the RPR (140). Binding of the RPP to the RPR also affects RPP solubility and proteostasis in the cell (141, 142).

The structure of the RPP revealed a cleft and FRET as well as other biochemical data suggested that the RPP interacts with N_{-8} - N_{-3} in the "single-stranded" 5′ leaders and influence the positioning of the 5′ leader in the RNase P-substrate complex [see also above and Fig. 1*A* (143–148)]. Binding the 5′ leader stabilizes the RNase P-substrate complex (143, 149). The length of the 5′ leader, however, varies with pre-tRNA identity; moreover, the length affects binding and the association rate constant, but not the cleavage rate constant [(138, 149), but see (150)]. These observations are consistent with *in vivo* data suggesting that the 5′ leader structure or length correlates with bacterial growth rate [(151), see also Chamberlain *et al.*, this issue]. Furthermore, the interaction of the RPP with the 5′ leader affects the affinity for metal ions necessary for cleavage. The interaction also compensates for structural differences among tRNA precursors by altering the energetic contributions to 5′ leader binding (138, 147, 152, 153).

Recent High Throughput Sequencing-Kinetics, HTS-Kin, data indicate that the *Eco* RPP facilitates the recognition of a consensus sequence in the pre-tRNA 5′ leaders [(154–156) and Chamberlain *et al.*, this issue]. Briefly, the identity of the N_{-3} and N_{-2} in the 5′ leader influences the selection of alternative substrates at the association step and not the cleavage step; also, the N_{-2} identity can influence the binding contribution of the RPP [(156, 157); see also below]. In addition, a sequence-favored interaction was reported between N_{-4} in the 5′ leader and the RNase P protein (158, 159). This finding may explain how substitution of a C to U at −4 in the 5′ leader of pre-$tRNA^{Tyr}$Su3 rescues the lower suppression efficiency caused by the G_{+2} to A_{+2} substitution (see below; Fig. 1*A*). Collectively, these data emphasized the importance of the pre-tRNA 5′ leader for correct and efficient RNase P processing and the contribution of RPP to the cleavage reaction.

Bacterial RPR: The "A_{248}–N_{-1}" interaction and residue N_{-2}

Examination of the bacterial tRNA gene sequences did not reveal any conserved sequences in 5′ leaders that could potentially interact with the RPR [see *e.g.* (154), and Chamberlain *et al.*, this issue]. However, in many bacteria, U_{-1} in pre-tRNA 5′ leaders (Fig. 1*A*) is the most abundant residue; in *E. coli*, roughly 60% have U_{-1}. The adenosine at position 248 (A_{248}; *E. coli* numbering; Fig. 2*A*) is conserved among bacterial RPRs and it has been suggested that A_{248} forms a Watson-Crick (WC) base pair with residue U_{-1} in the pre-tRNA leader (160, 161). Several *E. coli* precursors do not have U_{-1}. Also, in certain high GC-content bacteria, such as mycobacteria, C_{-1} is more frequent than U_{-1}, whereas in some other bacteria, G_{-1} and A_{-1} are also more abundant than U_{-1} (162). Moreover, WT *Eco* RPR cleave model hairpin-loop substrates having 3-methyl-U_{-1}, which interferes with the U_{-1} WC-surface, at the correct site [(163, 164); for a detailed analysis of the potential N_{-1}/N_{248} WC base pairing, see (164)]. Together, these data argue against WC-base pairing between N_{-1} (pre-tRNA) and A_{248} (RPR). In this context, the presence of a nucleobase at −1 is not required as suggested from studies of a model substrate but its absence results in aberrant cleavage and a reduction in the cleavage efficiency (76).

The bacterial RNase P-tRNA crystal structure represents the post-cleavage state and therefore provides no information about the interaction between N_{-1} and A_{248} in the RNase P-substrate ground-state complex (33). However, the Harris laboratory recently reported cryo-EM structures for *Eco* RNase P in complex with pre-tRNAs having U_{-1} (and A_{-2}) or G_{-1} (and G_{-2}) (37). The crystal and cryo-EM structures show that A_{248} stacks on the tRNA G_{+1}/C_{+72} bp (Fig. 3, *C* and *D*). This stacking interaction depends on the N_{-1} identity: for pre-tRNA with U_{-1} (and A_{-2}), A_{248} stacks on G_{+1}/C_{+72}, while for substrates with G_{-1} (and G_{-2}), A_{248} is positioned orthogonal relative to G_{+1}/G_{+72} (Fig. 3*D*). For the pre($A_{-2}U_{-1}$)-tRNA, A_{-2}, A_{333}, and G_{332} forms a continuous stack on U_{-1} (Fig. 3*D*). In the case of pre($G_{-2}G_{-1}$)-tRNA, G_{-1} appears to stack on the pre-tRNA G_{+1} with A_{333} and G_{332} stacking on G_{-2} (Fig. 3*D*). Moreover, the *Eco* RNase-pre-tRNA cryo-EM structures do not show WC pairing between N_{-1} and A_{248}.

In the bacterial RNase P-tRNA(-pre-tRNA) complexes, the Hoogsteen surface of A_{248} faces the 5′ termini of the tRNA [Fig 3, *C* and *D* (33, 37)]. Cross-linking and NAIM data indicate that the region at and near A_{248} interacts with the RPR and that the A_{248} Hoogsteen surface contributes to substrate binding (53, 165–169). This inference raises the possibility that N7 and the 6-NH_2 of A_{248} interact with chemical groups of N_{-1}. Consistent with this notion, the *Eco* RNase P-pre($A_{-2}U_{-1}$)-tRNA cryo-EM structure (37) suggests that the O4 of U_{-1} is positioned to form H-bonds with the A_{248} exocyclic amine. With G_{-1}, hydrogen bonding might be formed between O6 of G_{-1} and 6-NH_2 of A_{248} (Fig. 3*D*; see also Chamberlain *et al.*, this issue).

Changing G_{+2} to A_{+2} in the pre-$tRNA^{Tyr}$Su3 acceptor-stem reduced the level of matured tRNA *in vivo*, while a "second-site" mutation in the 5′ leader, C_{-4} to U_{-4} increased the tRNA levels five- to six-fold [Fig. 1*A* (8, 10, 20)]. Mutating G_{-2} and U_{-1} in pre-$tRNA^{Tyr}$Su3 to C_{-2} and A_{-1} did not change the cleavage site selection *in vivo* or *in vitro*. However, the resulting $tRNA^{Tyr}$Su3 suppressed UAG with ≈seven-fold lower

suppression efficiency than the "WT" $tRNA^{Tyr}Su3$ (170). Together, these findings indicate that structural changes in the pre-$tRNA^{Tyr}Su3$ 5′ leader can influence processing *in vivo* (see also Chamberlain *et al.*, this issue). Furthermore, *in vitro* studies revealed that the cleavage site varies depending on the identity of N_{-2} in the 5′ leader of pre-tRNAs and RPR type [type A *Eco* RPR and type B *Mycoplasma hyopneumoniae* RPR, *Hyo* RPR (171)]. Cleavage kinetics was also affected by the identity of the −2 residue in the substrate and with RPR type. Pre-tRNA with G_{-2} was cleaved with the lowest rate with the type B *Hyo* RPR, while the type A *Eco* RPR cleaved the U_{-2} pre-tRNA with the lowest rate (172). Hence, comparing *Eco* RPR (type A) and *Hyo* RPR (type B) reveals differences both with respect to cleavage site selection and cleavage rate (see also above). Also, for *Eco* RNase P, the G_{-2} in pre-$tRNA^{fMet}$ affects site selection and compensates for the negative impact by its WT C_{+1}/A_{+72} wobble bp (173, 174). Together, these *in vivo* and *in vitro* data identify N_{-2} as important for correct and efficient RNase P cleavage [see also (171)]. In this context, an *R*p-phosphorothioate modification at −2 in a $tRNA^{Gly}$ precursor interfered with cleavage by the *Bsu* RNase P holoenzyme indicating that it interacts, either indirectly (*via* a metal(II) ion) or directly with the enzyme (76). As discussed below, Mg^{2+} binds near the cleavage site (69, 175, 176). It is therefore conceivable that the N_{-2} nucleobase can influence the positioning/binding of Mg^{2+} and thereby impact substrate binding and/or catalysis (see also below).

Together, these data suggest that the stacking interactions at and near the cleavage site play important roles in anchoring the substrate where A_{248}, G_{332}, and A_{333} are part of a binding surface for N_{-2} and N_{-1} [(37), see also (53)]. The structural data further suggest that the architecture of this binding surface depends on the identities of N_{-2} and N_{-1} (Fig. 3*D*).

Chemical groups near the cleavage site and role of Mg^{2+}

Understanding the functions of different RNAs is tightly linked to deciphering the roles of metal ions such as Mg^{2+}; on average, there is one Mg^{2+} bound per 3 to 4 nucleotides [see *e.g.*, (177–179)]. Binding of metal ions affects RNA folding, RNA–RNA interactions, RNA–protein interactions, and catalysis. Their role in RNA folding has been covered in previous reviews (180, 181) and will not be discussed here. Here, we emphasize that bacterial RPR is folded into an active structure in a cooperative process that is completed at 5 to 10 mM Mg^{2+} [for reviews, see *e.g.*, (180, 181)].

As discussed above, RNase P activity with and without the protein subunit depends on the presence of metal(II) ions, that is, Mg^{2+}. Mg^{2+} affects the folding of the RPR and is involved in the chemistry of the cleavage reaction. For activity, however, Mg^{2+} can be replaced by other metal(II) ions such as Mn^{2+} and Ca^{2+} (177). Cleavage by RPR without the protein requires a higher concentration of metal(II) ions than when the RPP is present [see above (30, 182, 183); notably, addition of spermidine lowers the Mg^{2+} requirement in the RPR alone reactions (183)]. Under certain conditions, binding of metal(II) ions to an RNA cleaves the phosphodiester back bone by activating a neighboring 2′-OH as a nucleophile generating 5′-OH and 2′,3′-cyclic phosphate as cleavage products (184). Kazakov and Altman (175) showed that *Eco* RPR is cleaved by Mg^{2+} at five specific positions at pH 9.5, suggesting that these cleavage sites are in close proximity to where Mg^{2+} binds. Others have used Pb^{2+} to map metal(II) ion binding sites in both type A and type B RPRs and to probe the integrity of the RPR structure in response to changing residues in the RPR (185–187). Together, these studies placed Mg^{2+}-binding sites in the vicinity of where the tRNA TSL region interacts in the S-domain and where the pre-tRNA 3′ RCC-motif interacts with *Eco* RPR (P15 loop; Fig. 2*A*). Metal(II) ions were subsequently detected at these and other sites and at sites in the proximity of the tRNA 5′ end in the RNase P-tRNA crystal structure and the *Eco* RNase P-pre-tRNA cryo-EM structures [Figs. 2 and 3 (33, 37)].

Under certain conditions, Mg^{2+} also induces cleavage of pre-$tRNA^{Tyr}Su3$ between C_{-3} and G_{-2} in the 5′ leader, that is, at the junction of single- and double-stranded regions [Fig. 1*A* (175)]. Furthermore, based on the observed Mg^{2+}-induced cleavage of model substrates, in which the 2′-OH had been replaced by 2′-H at U_{-2}, C_{-1}, G_{+1}, and C_{+33} (C_{+33} in the AT1 model substrate corresponds to C_{+74} in pre-tRNA; Fig. 1*C*), it was suggested that the true substrate for *Eco* RPR has Mg^{2+} coordinated at the junction between the single- and double-stranded regions [Fig. 1*C* (72, 176)]. The structural topography of N_{+1}/N_{+72} also appears to influence binding metal(II)-ion(s) in the vicinity of the cleavage site (188, 189).

The 2′-OH at the cleavage site (at N_{-1}) is not required (190) but it influences different reaction steps. Substituting the 2′-OH at N_{-1} with 2′-H, 2′-F, or 2′-NH_2 in various RNA substrates, several laboratories have demonstrated that it (and its binding to Mg^{2+}) has a role in ground state binding of the substrate, cleavage site recognition/selection, and cleavage efficiency (55, 177). For example, *Eco* RPR-mediated cleavage of yeast $tRNA^{Phe}$ extended with a deoxyA_{-1} led to a lower cleavage rate with only a small effect on substrate binding compared to the unmodified substrate [steady state conditions (191)]. Smith and Pace suggested that ≥3 Mg^{2+} are bound near the cleavage site and are required for optimal cleavage (191). Replacing the N_{-1} 2′-OH group with 2′-H decreased the number of Mg^{2+} from three to two, indicating that this 2′-OH may be involved in binding Mg^{2+} during catalysis (see also above). Kazakov and Altman (175) suggested participation of two Mg^{2+} in the cleavage mechanism and two (rather than three) metal(II) ions were detected by cryo-EM and in the crystal structure near the cleavage site (see below).

Studies using *Bsu* RPR and a yeast pre-$tRNA^{Phe}$ with a five-nt-long 5′ leader also indicated the importance of the 2′-OH at position −1 for cleavage, both at the correct and alternative sites. In contrast, the 2′-OH at alternative cleavage sites does not significantly influence catalysis (91, 92). For *Eco* RPR, cleavage of model substrates with 2′-H (at N_{-1}) at the correct site does not affect mis-cleavage at the alternative site. This finding is consistent with the idea that the 2′-OH in the immediate vicinity of the cleavage site affects Mg^{2+} binding (163). However, a possible interaction of this 2′-OH with the RPR

cannot be excluded. This study also suggested a greater dependence on the 2′-OH at the cleavage site in the absence of the interaction between substrate residues +73 and 294 in the RPR (part of the "RCCA–RPR" interaction, see above). Moreover, it has been suggested that the 2′-OH at the cleavage site acts as an outer (or inner) sphere ligand for Mg^{2+} in the RNase P-substrate complex [(111, 112) see also (161)]. Evidence that the N_{-1} 2′-OH is involved in Mg^{2+} binding at the cleavage site is supported by data using substrates carrying a 2′-NH_2 at N_{-1}. The frequency of cleavage at N_{-1} vs N_{+1} (see Fig. 1) was shown to depend on pH; at pH 5.5, cleavage was detected at −1 while the cleavage site shifted to +1 with increasing pH. As discussed above, the presence of 2′-NH_3^+ at the cleavage site would interfere with Mg^{2+} binding (111, 112). The deprotonation of 2′-NH_3^+ at N_{-1} is also influenced by the identity of the +1/+72 bp in the substrate, indicating its role in positioning Mg^{2+} at the cleavage site [(189) see also (84, 164)]. Interestingly, in the *Eco* cryo-EM RNase P-pre($A_{-2}U_{-1}$)-tRNA structure, Ca^{2+} appears to be coordinated to the U_{-1} 2′-OH (37). Together, these data suggest that the N_{-1} 2′-OH is involved in binding/positioning Mg^{2+} near the cleavage site.

Two putative Mg^{2+} ions are positioned at the cleavage site in the yeast RNase P-pre-tRNA cryo-EM structure and both are coordinated to the *R*p-oxygen at the cleavage site (35; see also above). In the bacterial RNase P-tRNA crystal structure, two metal ions are also located near the matured 5′-end of the tRNA [Figs. 2 and 3 (33)]. Substitution with sulfur of either of the *R*p- or *S*p-oxygen at the cleavage site in pre-tRNAs led to slower cleavage rates by *Eco* RPR. Replacing Mg^{2+} with the "thiophilic" Cd^{2+} (or Mn^{2+}) rescues cleavage of the pre-tRNA with the *R*p-phosphorothioate modification (192–194). These data suggest a direct role of the *R*p-oxygen in coordinating Mg^{2+} at the cleavage site. In addition, residues in (and near) the P4-helix are close to the two metal ions positioned at the tRNA 5′ termini in the RNase P-tRNA crystal structure. The sequence of the P4-helix is well-conserved; P4 contains a metal(II)-binding site where a bulged U_{69} (Fig. 2) binds the catalytic metal ion. Cross-linking data suggested that U_{69} indeed interacts with the tRNA acceptor-stem; this "U_{69}-acceptor stem" interaction has been suggested to influence the affinity of catalytic metal ion(s) at the cleavage site through substrate positioning (195).

Substrate interaction, base stacking, and mechanism of RNase P cleavage

The "mature" tRNA structure is already adopted in the tRNA precursor (196, 197). As discussed above, the TSL region and the 3′ RCCA-motif interacts with RNase P and the length of the T- and acceptor-stem (12 bp-long in tRNAs) is suggested to act as a measuring device (for references, see above) that helps to determine the RNase P cleavage site. Continued base stacking involving bases both in TSL and TBS (Fig. 3*A*) together with the pairing between the tRNA "3′ RCCA-motif" and GGU sequence in the P15 loop anchors the substrate [Figs 2*D* and 3*C* (33, 164)]. Both A_{76} at the tRNA 3′ end and residue U_{257}, which corresponds to A_{295} in *Eco* RPR (Fig. 2*A*), stack on the "RCC-$U_{294}G_{293}G_{292}$-helix" (Fig. 3*B*). Moreover, the yeast $tRNA^{Phe}$ structure suggests that the discriminator base stacks on top of G_{+1}/C_{+72}, forming a structural unit (Fig. 3*C*, left panel). Formation of the "RCCA–RPR" interaction results in pairing of the discriminator base at position +73 in the tRNA and U_{294} and stacking of A_{248} on top of G_{+1}/C_{+72} in the RNase P-tRNA crystal and *Eco* RNase P-pre($A_{-2}U_{-1}$)-tRNA cryo-EM structures [Fig. 3, *C* and *D* (33, 37)].

These results suggest that base stacking plays an important role in stabilizing the RNase P-substrate interaction. In addition to its involvement in anchoring the substrate, it has been suggested that the stacking of A_{248} on top of the G_{+1}/C_{+72} bp acts as a cap. The cap would prevent water accessing the hydrophobic tRNA acceptor-stem and promoting nonspecific hydrolysis. The same expectation holds for the "RCCA–RPR interaction" [Fig. 3*B* (164)]. Moreover, in bacterial RPRs, A_{248} (*E. coli* numbering) is conserved and the stacking free energy for adenosine is more advantageous relative to G, C, and U (198). Recent data also suggest that WT *Eco* RPR_{A248} has the lowest activation energy barrier than *Eco* RPR variants with G, C, or U at position 248 (164). Collectively, these data provide a rationale for the conservation of A_{248} in bacterial (and some archaeal) RPR.

RNase P cleavage generates 3′-hydroxyl and 5′-phosphate products. Two metal(II) ions have been identified in the structures of various RNase P in complex with tRNA [post-cleavage states of bacterial, archaeal, and human RNase P (33, 35, 36) and with pre-tRNA yeast RNase P (34) and *Eco* RNase P (37)]. Irrespective of the RNase P source, two metal(II) ions are positioned near the 5′ end of the tRNA, suggesting a general two-metal-ion catalytic mechanism (Fig. 4*A*). However, before the structures became available, mechanistic models involving Mg^{2+} were presented based on available biochemical data and similarities to cleavage by other ribozymes and protein nucleases [see *e.g.*, (159, 175, 183, 191–193, 199–201). The combined biochemical and structural data led to the suggestion that the cleavage reaction proceeds through a pentacoordinate transition state. One metal(II) ion activates a water molecule that acts as the nucleophile (Me_A; Fig. 4*A*). The other metal(II) ion (Me_B) stabilizes the developing oxyanion in the transition state and might be involved in mediating the transfer of a proton resulting in a 3′-OH on the 5′ leader product. The conserved residue U_{69} (*Eco* RPR numbering; Fig. 2*A*) is implicated as playing a role in positioning the Mg^{2+} that generates the nucleophile, a model that is consistent with earlier biochemical and genetic data [Fig. 4*A*, see above and *e.g.* (159, 200, 201)]. As discussed above, the 2′-OH at N_{-1} in the substrate is also suggested to be involved in Me(II) ion binding (Me_B; Fig. 4*A*). The carbonyl oxygen (O2) at position 2 on the nucleobase (U_{-1} and C_{-1}) contributes to cleavage by *Eco* RPR. Modeling and the *E. coli* cryo-EM RNase P-pre($A_{-2}U_{-1}$)-tRNA complexes suggest that this O2 is exposed on the same surface as the N_{-1} 2′-OH (37, 76). This feature raises the possibility that this oxygen also contributes to binding of Me_B (76). In this scenario, however, the N_{-1} 2′-OH has to be prevented from acting as the nucleophile, as it would generate incorrect cleavage products with 5′-OH and 2′;3′-cyclic phosphate at

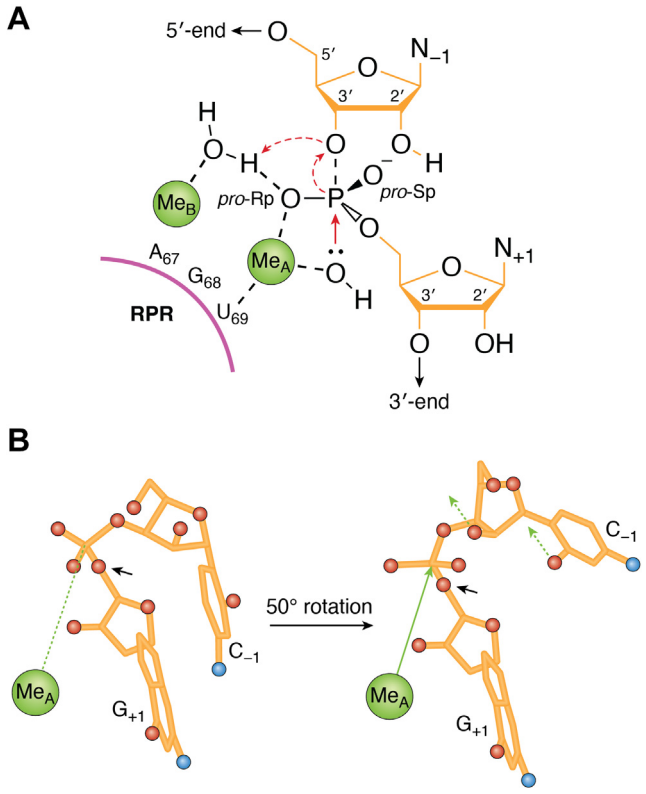

Figure 4. Models of the RNase P reaction mechanism. *A*, the model is adapted based on the models proposed by Liu *et al.* (201) and Wan *et al.* (36). The substrate (*orange*), the RPR (*magenta*), and metal(II) ions, Me_A and Me_B (*green*), are color coded as in Figures 1–3. The RPR numbering refers to *Escherichia coli* RPR, see Fig. 2*A*. The *solid red arrow* marks the nucleophilic attack on the phosphate, while the *dashed red arrows* mark the leaving 3′OH group and its protonation. *B*, model showing a 50° rotation of the P-O5′ phosphodiester bond (*blue arrow*) at the RNase P cleavage site, in a substrate with C_{-1} and G_{+1}, that position the Mg^{2+} that activates the water molecule for a nucleophilic attack on the phosphate as indicated (*solid green arrow*). The *green dashed arrows* mark the C_{-1} O2 and the 2′-OH groups, which are suggested to bind Mg^{2+} (see main text). These two groups are pointing in the same direction and both contribute to catalysis (76). The *red*- and *blue*-filled circles mark oxygens and exocyclic amines, respectively. Model adapted from Wu *et al.* (76).

their termini [(111, 112) see also (161)]. Modeling suggests that this outcome is achieved by the N_{-1} 2′-OH, pointing away from the scissile phosphate [Fig. 4*B*; for a detailed discussion (76)]. In this context, the N_{-1} 2′-OH is facing in a different orientation relative to the scissile phosphate in the *Eco* RNase P-pre-tRNA cryo-EM structures (37).

Processing of dimeric and multimeric precursor tRNAs and future challenges

Thus far, we have focused on the discussion of RNase P recognition and cleavage of monomeric precursors (*e.g.*, *E. coli* pre-$tRNA^{Tyr}$Su3 and model substrates). However, many bacterial tRNA gene transcripts carry more than one tRNA [see *e.g.*, (202, 203)]. In *E. coli*, most tRNA genes are clustered in co-transcribed units. Hence, an important task is understanding how RNase P recognizes tRNA transcripts with more than one tRNA sequence. Several ribonucleases in concert with RNase P trim these tRNA precursor transcripts, ultimately generating functional tRNAs. Among these enzymes, endoribonuclease E plays an important role in processing tRNA transcripts by cleaving in the leader and between tRNAs. The cleavage between tRNAs converts the pre-tRNA transcripts into smaller units, which RNase P and exoribonucleases subsequently target to generate functional tRNAs. As discussed above, a number of recent studies in *E. coli* suggest that RNase P is involved not only in generating the matured 5′ end of tRNAs but also plays an important role in separating individual pre-tRNA species from the larger primary transcripts for further processing [for reviews (204, 205), see also (206)].

The spacer regions between two tRNA genes vary in length: in *E. coli*, this distance ranges between 2 and 209 nucleotides (202, 207, 208). As discussed above, the T-even (*e.g.*, T4) *E. coli* bacteriophages encode tRNAs. Most of these sequences encode dimeric pre-tRNAs where the individual tRNAs are separated by less than five nucleotides. In the $tRNA^{Pro}$-$tRNA^{Ser}$ dimeric precursor of phage T4, neither tRNA contains the 3′ CCA sequence (Fig. 1*D*), and efficient RNase P processing was shown to prefer CCA at the 3′ end of $tRNA^{Ser}$ instead of having UAA (16, 209). The spacer between $tRNA^{Pro}$ and $tRNA^{Ser}$ is only 3 nt. The RPP interacts with residues at positions −8 to −3 in the 5′ leader sequences of monomeric pre-tRNAs, while residues −2 and −1 interact with the RPR [see above (138, 149, 210)]. So, how does bacterial RPP/RNase P interact with the leader given the proximity of $tRNA^{Pro}$ and the $tRNA^{Ser}$ RNase P cleavage site (see Fig. 1*D*)? This question is also relevant to uninfected cells. For example, *E. coli valT* and *lysW*, which are part of the larger "*lysT*" transcript carrying seven tRNAs (211), are only separated by 2 nt (including the 3′ ACCA sequence of the upstream $tRNA^{Val}$, *valT*, extends the spacer between *valT* and *lysW* to six nucleotides). The *in vivo* processing by RNase P of the "*lysT*" transcript is initiated by the removal of the ρ-independent transcription terminator located 3′ of the distal tRNA. Subsequently, RNase P processing proceeds in the 3′ to 5′ direction. Similar concerns pertain to other tRNA transcripts, such as those derived from the *valU* and *valV-valW* transcripts (211–213). *In vitro* data showed conclusively that the 3′ to 5′ processing by RNase P of the *valV-valW* transcript proceeds in a distributive manner (214). In this context, cleavage of a multimeric pre-tRNA by *Bsu* RPR was detected at the predicted sites (63).

It was suggested that *Eco* RPR (M1 RNA) forms dimers to carry out the RNase P reaction (183). Subsequently, it was reported that the *Bsu* RNase P holoenzyme form dimers, and it was discussed that the dimer form binds substrate differently compared to monomeric RNase P (215). The cryo-EM structure of the archaeal *Methanocaldococcus jannaschii* RNase P holoenzyme revealed a dimer (36, 216). Perhaps, dimerization of RNase P might be relevant to the general processing of dimeric and multimeric tRNA transcripts in bacteria. Nevertheless, how bacterial RNase P binds dimeric and multimeric pre-tRNAs is an open and interesting question that remains to be studied in more detail.

RNase P also processes other RNAs, such as pre-tmRNA, pre-4.5S RNA, tRNA-like (pseudo-knot) structures present at the 3′ end of certain plant RNA virus genomes, bacteriophage M3 RNA, bacteriophage-derived antisense C4 RNA, *E. coli*

non-coding RNAs transcribed from intergenic regions, transient structures in riboswitches, and mRNAs [(102, 217–225), for reviews, see refs (54, 226)]. Altman *et al.* were the first to report in 1990 that an mRNA (T4 gene 32) is an RNase P substrate (227). It has recently been suggested that RNase P is involved in mRNA metabolism more broadly (225, 226). These studies are at an early stage and raise many questions such as cleavage site recognition and possible link to ribosome binding and initiation of translation. Interestingly, there is some evidence that the dimeric form of *Bsu* RNase P primarily interacts with the 30S ribosomal subunit, forming an RNase P–30S ribosome complex (228). Also, RNase P was suggested to be associated with RNA degradosome subunits in yeast mitochondria (229). This finding raises the question of whether RNase P interacts with the RNA degradosome in bacteria (230). Ongoing studies in bacteria that investigate the role of RNase P and RNA/mRNA processing using modern technologies such as RNA-Seq will likely provide new and exciting findings that will increase our insight into the biological roles of RNase P (224, 225).

Gene-targeting technology based on RNase P and M1 RNA: Making use of the unexpected

Gene-targeting strategy based on RNase P: External guide sequence

Altman's early studies on substrate recognition by M1 RNA and RNase P led to the concept of "external guide sequence" (EGS) that could be used for targeted RNA cleavage (190, 231). In this strategy, a custom-designed EGS can guide M1 RNA and RNase P to cleave any mRNA in a sequence-specific manner, provided that the EGS hybridizes to the mRNA and forms a tRNA-like structure [Fig. 5, *A–C* (190)]. Two components of an EGS are important for its functions (231). First, the EGS should have a "targeting sequence," which is complementary to the mRNA target and binds to the mRNA substrate through base-pairing interactions. Second, the EGS should also contain an "RNase P–recognized sequence," which resembles a portion of the T-loop and stem and the variable loop and stem of a pre-tRNA. This second sequence enhances the interaction between the EGS and RNase P (and M1 RNA) and is crucial for efficient cleavage of the targeted mRNA by RNase P and M1 RNA (232).

Different designs and constructions have been explored to generate various EGSs for RNase P-EGS applications. For example, Werner *et al.* reported successful construction of short EGSs (233). In the EGS–mRNA complex under this design, the EGS consists of only 15 to 20 nt and resembles the 3′ acceptor stem and 3′ TSL regions, and the targeted mRNA resembles the 5′ leader sequence, 5′ acceptor stem, the variable region, and the 5′ TSL of a tRNA (Fig. 5*A*). Another design of EGS links an EGS covalently to M1 RNA, to generate a sequence-specific ribozyme, called M1GS RNA (Fig. 5, *D* and *E*), that can cleave any mRNA substrate that hybridizes with the guide sequence [see below (234)].

Gene-targeting strategy based on M1GS ribozyme

Investigations by the Altman laboratory showed that M1GS RNA is active and efficient in cleaving numerous mRNAs (234). M1GS RNA is also easy-to-make and could be generated by adding a guide sequence to the 3′ end of M1 RNA (235).

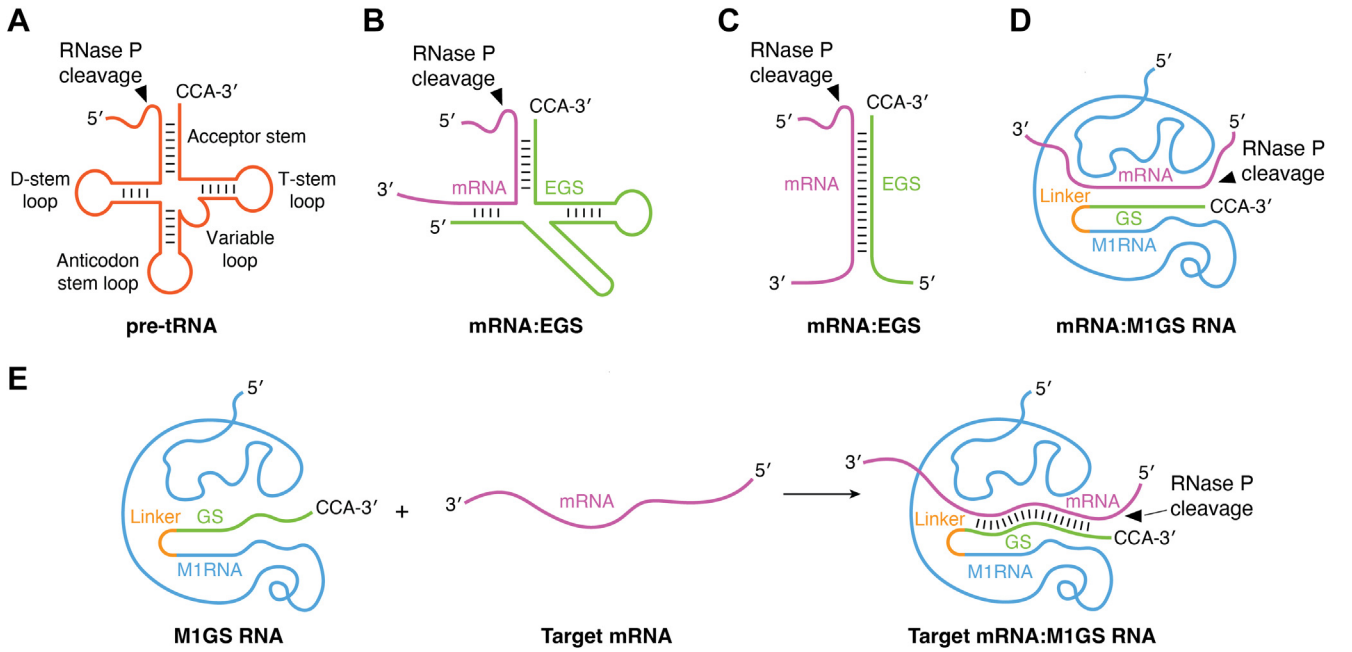

Figure 5. Representation of various RNase P substrates. Gene-targeting strategies based on RNase P and M1 RNA with their associated external guide sequences (EGSs) (*A–C*). A hybridized complex (*B*) of a target RNA (in *red*, *e.g.* mRNA) and an EGS (in *green*) that resembles a part of the structure of a tRNA structure (*A*) can be cleaved by RNase P and M1 RNA. Substrates in (*A*) and (*B*) can be cleaved by human RNase P and M1 ribozyme. In contrast, the stem structure in (*C*) can only serve as a substrate for M1 RNA and cannot be cleaved by human RNase P. *D*, an M1GS ribozyme–mRNA substrate complex. *E*, binding process of an M1GS ribozyme (in *blue*) with a target mRNA substrate (in *red*). The arrow shows the site of the cleavage by RNase P and M1 RNA.

The guides should contain a "targeting sequence," which hybridizes to the mRNA target. In addition, the guide sequence should contain an unpaired 3′-NCCA end as present in natural *E. coli* pre-tRNA substrates in order to allow efficient cleavage by the tethered M1 RNA (Fig. 5, *D* and *E*). In the M1GS design, the guide sequence binds to its target mRNA and directs M1 RNA, which is in proximity due to the covalent attachment to the guide sequence, to the cleavage site (Fig. 5*E*). Subsequent studies in the Altman laboratory demonstrated that M1GS RNA can block gene expression in bacteria and virus-infected mammalian cells (Table 1) (234, 236). Further studies showed that M1GS ribozymes cleaved numerous cellular and viral mRNA targets in human cells and in diminishing viral infection in animals (Table 1) [see below and review (235)].

In principle, the guide sequence can be tethered to different regions of M1 RNA in addition to the 3′ end of M1 RNA. In their studies with an M1 RNA tethered with a pre-tRNA substrate adjacent to the M1 RNA region for substrate binding, Pace *et al*. demonstrated that an M1 RNA tethered with a 3' region of a tRNA could cleave an RNA substrate resembling the 5′ region of a tRNA including the 5' leader sequence and the 5′ region of the acceptor stem, when the RNA substrate base-paired with the tethered tRNA sequence (237). However, it is unclear whether such customized ribozymes are capable of cleaving mRNA targets and modulating their expression in cultured cells.

The successful use of M1GS ribozyme and the EGSs associated with bacterial and human RNase P in modulating gene expression in different organisms and cells (Table 1) truly reflect Altman's impact and contribution to the development of RNase P as a tool in both basic research and clinical applications.

The RNase P–associated EGS and M1GS ribozymes represent a class of RNA-based gene targeting agents for gene interference and gene-editing applications, which include conventional antisense molecules (238), ribozymes derived from the hammerhead, hairpin, and group I intron ribozymes (239–241), siRNAs (242), and CRISPR/Cas-associated gRNAs (243). Collectively, these methods lay the foundation for the current widespread use of RNA as a tool to modulate gene expression and as a medicine for clinical applications (244).

Applications of RNase P as a tool for basic research and for therapy

With the EGS technology, Altman *et al*. successfully modulated the expression of essential genes of several bacteria, including *Salmonella typhimurium*, *Klebsiella pneumoniae, Mycobacterium smegmatis, Staphylococcus aureus*, and *Francisella tularensis* and achieved an antimicrobial effect for the infections of several pathogenic bacteria (Table 1) (245). Furthermore, the RNase P-EGS technology effectively inhibited gene expression and development of *Plasmodium falciparum*, the causative agent of malaria (Table 1) (246). The constructed EGSs appeared to be highly specific and were capable of species-specific targeting.

Altman *et al*. also developed EGSs of different designs using various modifications including morpholino modifiers (245).

Table 1
Representative examples of studies using RNase P ribozymes and the EGS technology against targets associated with human diseases

Target	Method	Effects	Cell/animal model	References
Virus (human influenza virus)	EGS (vector expressed)	Inhibiting viral gene expression and replication	Cultured cells	(249)
Virus (hepatitis B virus)	M1GS and EGS (vector expressed)	Inhibiting viral gene expression and growth and reducing disease progression in animals	Cultured cells and mice	(247, 254, 262)
Virus (HIV)	EGS (vector expressed)	Inhibiting viral gene expression and replication of multiple HIV clades	Cultured cells	(274, 275)
Virus (human cytomegalovirus and herpes simplex virus 1)	M1GS and EGS (vector expressed)	Inhibiting viral gene expression and growth	Cultured cells	(234, 250, 251, 276–279)
Virus (murine cytomegalovirus)	M1GS and EGS (vector expressed)	Inhibiting viral gene expression and growth and reducing disease progression in animals	Cultured cells and mice	(257, 258, 266, 280)
Virus (Kaposi Sarcoma Associated Herpesvirus)	M1GS (vector expressed) and EGS (chemically synthesized)	Inhibition viral gene expression and growth	Cultured cells	(248, 252)
Bacterium (*Escherichia coli*)	EGS (vector expressed and chemically synthesized)	Blocking bacterial gene expression and growth	Cultured bacteria	(236, 281–283)
Bacteria (*Salmonella typhimurium, Klebsiella pneumoniae, Mycobacterium* spp., and *Acinetobacter*)	EGS (chemically synthesized)	Blocking bacterial gene expression and growth	Cultured bacteria	(265, 282–285)
Bacterium (*Staphylococcus aureus*)	EGS (chemically synthesized)	Blocking bacterial gene expression and growth and reducing disease progression in animals	Cultured bacteria and mice	(282, 284, 285)
Protozoan (*Plasmodium falciparum*)	EGS (chemically synthesized)	Blocking parasitic gene expression and growth	Cultured protozoan	(245, 286)
Human (BCR-ABL oncogene)	M1GS (vector expressed)	Decreasing the target mRNA expression and preventing the function of the BCR-ABL oncogenes	Cultured cells	(263)
Human (PKC and bcl-xL)	EGS (chemically synthesized)	Decreasing the target mRNA expression and blocking the function of the targets	Cultured cells	(264)
Human (CCR5)	M1GS and EGS (vector expressed)	Blocking CCR5 expression and HIV infection	Cultured cells	(287, 288)

Furthermore, EGSs could be expressed using expression vectors in bacteria or chemically synthesized and conjugated with a cell-penetrating peptide for direct delivery. If EGS technology can be used in antimicrobial therapy, its ability to achieve species-specific inhibition of bacterial viability could become very useful in circumventing the current limitation of narrow spectrum antimicrobials in inhibiting commensal nonpathogenic bacteria. These results by Altman *et al.* showed the promise of applying EGS technology for antibacterial therapy (245).

Altman's initial work on EGS generated great interest and excitement in developing the EGS technology for antiviral applications (Table 1). His laboratory and numerous laboratories around the world had demonstrated that RNase P and M1GS RNA were effective in blocking infections of HIV, human influenza virus, hepatitis B virus and four herpesviruses including human and murine cytomegalovirus (MCMV), herpes simplex virus 1, and Kaposi's sarcoma-associated herpesvirus (42, 235, 247, 248).

Among the first antiviral EGS studies, Plehn-Dujowich *et al.* constructed EGSs against the mRNAs coding for the nucleocapsid protein and polymerase of human influenza virus (249). They further showed that targeting two different mRNAs simultaneously by the EGS technology appeared to reduce viral growth more than targeting of a single mRNA. In their EGS studies against HIV, which infects CD4 T cells and decreases their levels *in vivo*, Hnatyszyn *et al.* showed that RNase P effectively blocked HIV gene expression and replication (275).

Liu *et al.* showed that RNase P–associated EGS RNAs and M1GS ribozymes were also highly active in targeting the mRNAs of herpes simplex virus 1 and human cytomegalovirus *in vitro* and blocking the gene expression and replication of these viruses in cultured cells (250, 251). Furthermore, they demonstrated that exogenous administration of chemically synthesized 2′-*O*-methyl-modified EGS to Kaposi's sarcoma-associated herpesvirus–infected human primary-effusion lymphoma cells significantly inhibited viral expression and growth (252).

Studies were also carried out to investigate the activity of EGSs and M1GS ribozymes for modulating gene expression and blocking viral infection in mice (Table 1). In one study, M1GS ribozyme-expression plasmid constructs were delivered in mice using a hydrodynamic transfection procedure (253). Expression of M1GS ribozymes were found in the spleens and livers and blocked gene expression and infection of MCMV *in vivo*. The delivery of M1GS expression constructs led to the inhibition of MCMV pathogenesis and prolonged the survival of the infected mice (253). In another study, the EGS expression constructs were delivered using a *Salmonella*-based vector into mice (254). The delivery of the EGS expression constructs effectively blocked the gene expression and replication of hepatitis B virus (HBV) *in vivo* (254).

To develop better EGSs, Yuan and Altman employed *in vitro* selection procedures for generating variant EGSs that were more efficient in inducing human RNase P cleavage of a target mRNA than the EGS derived from a natural tRNA sequence (232). Similarly, to further enhance the efficiency of ribozymes, *in vitro* selection procedures were used to select for M1GS variants that efficiently cleaved an mRNA (255). These efforts led to the development of numerous M1GS ribozyme variants that cleave their mRNA substrates more efficiently than the M1GS ribozyme derived from the M1 RNA sequence (235, 256). Importantly, when expressed in cultured cells and in mice, the EGS and M1 ribozyme variants selected *in vitro* were more effective in blocking viral gene expression and infection than the EGS derived from a natural tRNA sequence and the M1GS ribozyme derived from the WT M1 RNA sequence, respectively (255, 257–262).

In using the EGS technology in anti-tumor applications, Sánchez-García and colleagues constructed M1GS ribozymes to hydrolyze chimeric RNAs originating from chromosomal abnormalities (263). M1GS RNAs appeared to be highly specific and only cleaved the target chimeric mRNA *in vitro*. Furthermore, expression of the constructed RNase P ribozymes inhibited the oncogenic effect of BCR-ABL function in cultured mammalian cells (263).

In another study, Stein et al. generated EGSs to induce RNase P–mediated cleavage of the mRNA that encodes protein kinase C-α and antiapoptotic protein bcl-xL (264). They administered chemically synthesized 2′-O-methyl–modified EGSs into T24 bladder carcinoma cells for specific downregulation of protein kinase C-α and bcl-xL expression. They did not observe any nonspecific cleavage, which is usually associated with RNase H–based methods (264). These experiments provided direct evidence that RNase P–mediated cleavage induced by EGS is highly specific in targeting its mRNA. Collectively, these results suggested a general applicability of the EGS technology for anticancer applications (264).

Highly active RNase P ribozymes and EGSs were generated using *in vitro* evolution approaches (42, 235). Some of these molecules were highly effective in blocking gene expression in cultured cells and in mice. Biochemical characterization suggested that the mutations found in the selected ribozyme variants enhance the rate of cleavage and improve binding to specific mRNA regions, which are not present in pre-tRNAs (251, 255). Similar studies showed that the selected EGSs increased their targeting activity by increasing tertiary interactions affecting folding of the mRNA–EGS complex into a tRNA-like structure in addition to enhancing the interactions of the EGSs with RNase P (236, 256). These promising results have laid the foundation for developing better and more active RNase P ribozymes and EGSs for gene-targeting applications.

Advantage and disadvantage of the RNase P ribozyme and EGS technology

Traditional antisense technology employs cellular RNase H to degrade the mRNA target (238). However, nonspecific cleavage at non-targeted sites is a potential problem, as RNase H does not require a 100% complementary duplex for direct cleavage of the target mRNA (238). Compared to conventional antisense DNA and RNA, M1GS ribozyme can be highly

specific in cleaving its targeted mRNA (235, 263). For example, Sanchez-Garcia et al. showed that M1GS ribozyme can be specific in cleaving one substrate over another even though the two substrates share the first nine contiguous base pairs complementary to the guide sequence (263). In another study using short EGSs complementary to their target sequences to induce endogenous RNase P holoenzyme to cleave their targets and reduce bacterial viability in *E. coli*, three nucleotides unpaired out of a 15-mer EGS still favor complete inhibition of bacterial viability by the EGS but five unpaired nucleotides do not (265, 281-284). These interesting observations suggested that the targeting specificity of M1GS ribozyme may not be the same as that of the EGS when it is separated from M1 RNA or the holoenzyme *in vitro*. Furthermore, they implied that the sequence specificity of M1GS ribozymes in the presence of various proteins in human cells is perhaps different from that of the EGS interacting the bacterial holoenzyme and other proteins in *E. coli*. Additional studies on these issues, especially the specificity of M1GS ribozymes and EGS coupled with RNase P in human cells, should provide insight into the mechanism of how they achieve sequence specificity for targeting and facilitate the development of highly specific EGSs and M1GS ribozymes for therapeutic applications.

Compared to other ribozymes including hammerhead and hairpin ribozymes, M1GS ribozyme possesses several unique features as a gene-targeting tool. First, M1GS ribozyme can fold into a defined active conformation in the absence of its substrates. Second, while M1GS can cleave any designed sequence, hammerhead and hairpin ribozymes are limited by the requirement for the presence of specific nucleotide sequence (–GUX–) in the target mRNA for the cleavage to occur (239–241). Furthermore, a single point mutation in the required GUX sequence could render the ribozymes ineffective for target mRNA cleavage. The low specific sequence requirements at the cleavage site provide M1GS ribozyme with better flexibility to be used against almost any target, including positionally fixed target sites such as the fusion junction of two chromosomes resulting in an oncogenic chimeric mRNA (263). Third, the small ribozymes may have the disadvantage to be either rather inefficient under physiological conditions (*e.g.*, in the case of the minimal hammerhead ribozymes) or to catalyze ligation quite efficiently (*e.g.*, in the case of natural hammerhead ribozymes or the hairpin ribozymes); ligation will limit the efficiency of target cleavage, a clear disadvantage relative to RNase P and M1GS RNAs, which do not catalyze the reverse reaction.

Compared to other nucleic acid–based gene interference approaches, the EGS technology with the use of endogenous human RNase P exhibits several unique and attractive features as a gene-targeting tool. First, the mechanism of the EGS technology is different from other nucleic acid–based gene-targeting approaches in degrading the target mRNA. The EGS technology uses endogenous RNase P, which is one of the most ubiquitous, stable, and efficient enzymes in all types of cells (42, 245). This essential enzyme is highly expressed and is responsible for the processing of all tRNA precursors that account for approximately 2% of total cellular RNA. The action of RNase P in the presence of the EGS will result in irreversible cleavage of the target mRNA in a highly efficient catalytic fashion.

Second, the sequence specificity of the EGS technology is governed by two different types of interactions between the EGS and the target mRNA: (i) the base-pairing interactions in which the sequence of 12 nt in the EGS hybridizes with the target mRNA and (ii) the interactions between the target mRNA and the other part of the EGS sequence (equivalent to the T-stem and T-loop and variable regions of a tRNA) which are required for folding of the RNase P–recognizable tertiary structure (235). Thus, the EGS-based technology is highly specific and does not generate nonspecific "irrelevant cleavage" that is observed in RNase H–mediated cleavage induced by conventional antisense phosphorothioate molecules (252, 266). Third, cells expressing these molecules for more than 40 days appear to be normal indicating that EGSs exhibit little sign of cytotoxicity (250–252, 264).

In recent years, the use of the RNA interference (RNAi) approach to degrade mRNA associated with human diseases has been the focus for nucleic acid–based gene interference studies and several compounds based on RNAi have been approved for clinical therapy against specific human diseases (242). RNAi has the advantage of utilizing the cellular machinery in its process to knockdown mRNA and can be effective in small concentration. However, the siRNA technology may "sequester or misguide" a cellular machinery which may have consequences for cell function not foreseeable at present. More recently, genome-editing approaches such as those with CRISPR/Cas-associated gRNAs (243) have shown promising results for potential clinical applications.

Studies comparing the effects of the RNase P–based gene-targeting approach with those of other RNA-based methods have not been extensively performed. Results from Hayday *et al.* showed that shRNA and native tRNA-derived EGSs could both target the thymosin beta gene in cultured cells, but the extent of RNA reduction with shRNA was significantly greater (266, 267). More studies are needed to compare the activity and effectiveness of M1GS RNA/the EGS technology and RNAi and CRISPR-Cas–based approaches for modulating gene expression in human cells.

As with any gene therapy design, stability and delivery of the agents remain a big concern. The delivery problem affects the siRNA technology to the same extent as the EGS technology. For stability, the ribozymes and EGSs could be chemically synthesized with 2′ hydroxyl modification and/or phosphorothioates to resist cellular endonucleases (244). As an alternative to the viral vector approach, smaller ribozymes can be delivered *ex vivo* by encapsulating them in liposomes or other biodegradable polymeric matrix (244, 252, 264). Endogenous and stable expression of M1GS ribozyme by viral vectors remains one of the most practical choices for M1GS expression and delivery. EGSs are small molecules of 25 to 60 nucleotides. Therefore, the EGSs can be easily synthesized and modified

chemically (244, 252, 264). Thus, an EGS can be delivered directly (in naked form or with the aid of liposomes) to cells as well as delivered by expression vectors such as retroviral vectors.

Future directions and challenges

RNase P–associated EGS and M1GS ribozyme represent promising gene-targeting agents for both basic research and clinical applications. They are unique due to the use of RNase P and its catalytic RNA. Thus, the RNase P–based technology can complement other RNA-based gene-targeting approaches including those with conventional antisense molecules, ribozymes derived from the hammerhead, hairpin, and group I-intron ribozymes, RNA interference, and CRISPR/Cas gene editing methods. Future studies may be needed to address several challenges and develop these agents with the following considerations. The cleavage efficiency and specificity of the RNase P guide sequence technology *in vivo* will be further improved by better design and construction of EGSs and M1GS ribozymes including those selected *in vitro*. Moreover, the delivery and expression of the EGS and M1GS ribozymes can be optimized with the recently developed novel vectors and lipid carrier methods that have been shown to be successful for clinical applications (244, 268). These studies will facilitate the development of the RNase P guide sequence technology in clinics for treatment of various human diseases including infections and cancers.

Acknowledgments—The authors acknowledge the work of researchers who have contributed to the understanding of RNase P and the funding agencies that have supported the author's research. Gratitude also goes to Dr L. Lai and Ms T. Bergfors for critical reading of the manuscript and T. Lin for critical reading and editorial assistance. Dr V. Gopalan is recognized for constructive comments on the manuscript. We also acknowledge the work that has not been referred to but for references see indicated reviews in the main text.

Author contributions—L. A. K., F. L., and W. H. M. writing–review and editing; L. A. K., F. L., and W. H. M. writing–original draft; L. A. K., F. L., and W. H. M. conceptualization.

Funding and additional information—Work in the L. A. K. laboratory was supported by the Swedish Research Council (N/T) and the Uppsala RNA Research Center (Swedish Research Council Linneus support), W. H. M. laboratory was supported by NIH extramural grants AI10257, AI00020, and GM42123. The work in the F. L. laboratory was supported by NIH grants AI041927 and DE14812 and a University of California Start-Up Fund. The content is solely the responsibility of the authors and does not necessarily represent the official views of the National Institutes of Health.

Conflict of interest—The authors declare that they have no conflicts of interest with the contents of this article.

Abbreviations—The abbreviations used are: EGS, external guide sequence; LMB, Laboratory of Molecular Biology; MCMV, murine cytomegalovirus; NAIM, nucleotide analog interference mapping; RNAi, RNA interference; TBS, TSL binding site; TSL, T-stem loop; WC, Watson-Crick.

References

1. Crick, F. H. (1958) On protein synthesis. *Symp. Soc. Exp. Biol.* **12**, 138–163
2. Watson, J. D. (2007) *Avoid Boring People: Lessons from a Life in Science.* Oxford University Press, Oxford New York, 112
3. Hoagland, M. B., Stephenson, M. L., Scott, J. F., Hecht, L. I., and Zamecnik, P. C. (1958) A soluble ribonucleic acid intermediate in protein synthesis. *J. Biol. Chem.* **231**, 241–257
4. Tiessières, A. (1959) Some properties of soluble ribonucleic acid from Escherichia coli. *J. Mol. Biol.* **1**, 365–374
5. Allen, E. H., and Schweet, R. A. (1960) Role of transfer ribonucleic acid in hemoglobin synthesis. *Biochim. Biophys. Acta* **39**, 185–187
6. Holley, R. W., Everett, G. A., Madison, J. T., Marquisee, M., Merrill, S. H., Penswick, J. R., *et al.* (1965) Structure of a ribonucleic acid. *Science* **147**, 1462–1465
7. Goodman, H. M., Abelson, J., Landy, A., Brenner, S., and Smith, J. D. (1968) Amber suppression: a nucleotide change in the anticodon of a tyrosine transfer RNA. *Nature* **217**, 1019–1024
8. Smith, J. D., Barnett, L., Brenner, S., and Russell, R. L. (1970) More mutant tyrosine transfer ribonucleic acids. *J. Mol. Biol.* **54**, 1–14
9. Altman, S. (1971) Isolation of tyrosine tRNA precursor molecules. *Nat. New Biol.* **229**, 19–21
10. Altman, S., and Smith, J. D. (1971) Tyrosine tRNA precursor molecule polynucleotide sequence. *Nat. New Biol.* **233**, 35–39
11. Burdon, R. H. (1967) Molecular configuration of cytoplasmic transfer RNA precursors. *J. Mol. Biol.* **30**, 571–573
12. Lal, B. M., and Burdon, R. H. (1967) Maturation of low molecular weight RNA in tumour cells. *Nature* **213**, 1134–1135
13. Bernhardt, D., and Darnell, J. E. (1969) tRNA synthesis in Hela cells: a precursor to tRNA and the effects of methionine starvation on tRNA synthesis. *J. Mol. Biol.* **42**, 43–56
14. McClain, W. H., Guthrie, C., and Barrell, B. G. (1972) Eight transfer RNAs induced by infection of Escherichia coli with bacteriophage T4. *Proc. Natl. Acad. Sci. U. S. A.* **69**, 3703–3707
15. Deutscher, M. P., Foulds, J., and McClain, W. H. (1974) Transfer ribonucleic acid nucleotidyl-transferase plays an essential role in the normal growth of Escherichia coli and in the biosynthesis of some bacteriophage T4 transfer ribonucleic acids. *J. Biol. Chem.* **249**, 6696–6699
16. Seidman, J. G., and McClain, W. H. (1975) Three steps in conversion of large precursor RNA into serine and proline transfer RNAs. *Proc. Natl. Acad. Sci. U. S. A.* **72**, 1491–1495
17. Robertson, H. D., Altman, S., and Smith, J. D. (1972) Purification and properties of a specific Escherichia coli ribonuclease which cleaves a tyrosine transfer ribonucleic acid precursor. *J. Biol. Chem.* **247**, 5243–5251
18. Schedl, P., and Primakoff, P. (1973) Mutants of Escherichia coli thermosensitive for the synthesis of transfer RNA. *Proc. Natl. Acad. Sci. U. S. A.* **70**, 2091–2095
19. Sakano, H., Yamada, S., Ikemura, T., Shimura, Y., and Ozeki, H. (1974) Temperature sensitive mutants of Escherichia coli for tRNA synthesis. *Nucl. Acids Res.* **1**, 355–371
20. Smith, J. D. (1976) Transcription and processing of transfer RNA precursors. *Prog. Nucl. Acid Res. Mol. Biol.* **16**, 25–73
21. McClain, W. H. (1977) Seven terminal steps in a biosynthetic pathway leading from DNA to transfer RNA. *Acc. Chem. Res.* **10**, 418–425
22. Kole, R., and Altman, S. (1981) Properties of purified ribonuclease P from Escherichia coli. *Biochemistry* **20**, 1902–1906
23. Guerrier-Takada, C., Gardiner, K., Marsh, T., Pace, N., and Altman, S. (1983) The RNA moiety of ribonuclease P is the catalytic subunit of the enzyme. *Cell* **35**, 849–857
24. Guerrier-Takada, C., and Altman, S. (1984) Catalytic activity of an RNA molecule prepared by transcription *in vitro*. *Science* **223**, 285–286
25. McClain, W. H., Lai, L. B., and Gopalan, V. (2010) Trial, travails and triumphs: an account of RNA catalysis in RNase P. *J. Mol. Biol.* **397**, 627–646

26. Kruger, K., Grabowski, P. J., Zaug, A. J., Sands, J., Gottschling, D. E., and Cech, T. R. (1982) Self-splicing RNA: Autoexicision and Autocyclization of the ribosomal RNA intervening sequence of Tetrahymena. *Cell* **31**, 147–157
27. Rich, A. (1962) Horizons in biochemistry. In: Kasha, M., Pullman, B., eds. *On the Problems of Evolution and Biochemical Information Transfer*, Academic Press, New York: 103–126
28. Gilbert, W. (1986) The RNA world. *Nature* **319**, 618
29. Liu, F., and Altman, S. (2010). In *Ribonuclease P. Protein Reviews 2010* **10**. Springer, New York, Dordrecht, Heidelberg, London
30. Pannucci, J. A., Haas, E. S., Hall, T. A., Harris, J. K., and Brown, J. W. (1999) RNase P RNAs from some Archaea are catalytically active. *Proc. Natl. Acad. Sci. U. S. A.* **96**, 7803–7808
31. Pulukkunat, D. K., and Gopalan, V. (2008) Studies of Methanocaldococcus jannaschii RNase P reveal insights into the roles of RNA and protein cofactors in RNase P catalysis. *Nucleic Acids Res.* **36**, 4172–4180
32. Kikovska, E., Svärd, S. G., and Kirsebom, L. A. (2007) Eukaryotic RNase P RNA mediates cleavage in the absence of protein. *Proc. Natl. Acad. Sci. U. S. A.* **104**, 2062–2067
33. Reiter, N. J., Osterman, A., Torres-Larios, A., Swinger, K. K., Pan, T., and Mondragón, A. (2010) Structure of a bacterial ribonuclease P holoenzyme in complex with tRNA. *Nature* **468**, 784–789
34. Lan, P., Tan, M., Zhang, Y., Niu, S., Chen, J., Shi, S., *et al.* (2018) Structural insight into precursor tRNA processing by yeast ribonuclease P. *Science* **362**, eaat6678
35. Wu, J., Niu, S., Tan, M., Huang, C., Li, M., Song, Y., *et al.* (2018) Cryo-EM structure of the human ribonuclease P holoenzyme. *Cell* **175**, 1393–1404
36. Wan, F., Wang, Q., Tan, J., Tan, M., Chen, J., Shi, S., *et al.* (2019) Cryo-electron microscopy structure of an archaeal ribonuclease P holoenzyme. *Nat. Commun.* **10**, 2617
37. Zhu, J., Huang, W., Zhao, J., Huynh, L., Taylor, D. J., and Harris, M. E. (2022) Structural and mechanistic basis for recognition of alternative tRNA precursor substrates by bacterial ribonuclease P. *Nat. Commun.* **13**, 5120
38. Jarrous, N., and Gopalan, V. (2010) Archaeal/Eukaryal RNase P: subunits, functions and RNA diversification. *Nucl. Acids Res.* **38**, 7885–7894
39. Samanta, M. P., Lai, S. M., Daniels, C. J., and Gopalan, V. (2016) Sequence analysis and comparative study of the protein subunits of archaeal RNase P. *Biomolecules* **6**, 22
40. Kimura, M. (2017) Structural basis for activation of an archaeal ribonuclease P RNA by protein cofactors. *Biosci. Biotechnol. Biochem.* **81**, 1670–1680
41. Phan, H. D., Lai, L. B., Zahurancik, W. J., and Gopalan, V. (2021) The many faces of RNA-based RNase P, an RNA-world relic. *Trends Biochem. Sci.* **46**, 976–991
42. Jarrous, N., and Liu, F. (2023) Human RNase P: overview of a ribonuclease of interrelated molecular networks and gene-targeting systems. *RNA* **29**, 300–307
43. Altman, S., Bothwell, A. L., and Stark, B. C. (1975) Processing of E. coli tRNA Tyr precursor RNA *in vitro*. *Brookhaven Symp. Biol.*, 12–25
44. Leon, V., Altman, S., and Crothers, D. M. (1977) Influence of the A15 mutation on the conformational energy balance in Escherichia coli tRNA Tyr. *J. Mol. Biol.* **113**, 253–265
45. Kirsebom, L. A., Baer, M. F., and Altman, S. (1988) Differential effects of mutations in the protein and RNA moieties of RNase P on the efficiency of suppression by various tRNA suppressors. *J. Mol. Biol.* **204**, 879–888
46. Kirsebom, L. A., and Altman, S. (1989) Reaction *in vitro* of some mutants of RNase P with wild-type and temperature-sensitive substrates. *J. Mol. Biol.* **207**, 837–840
47. Guthrie, C., Seidman, J. G., Altman, S., Barrell, B. G., Smith, J. D., and McClain, W. H. (1973) Identification of tRNA precursor molecules made by phage T4. *Nat. New Biol.* **246**, 6–11
48. Moen, T. L., Seidman, J. G., and McClain, W. H. (1978) A catalogue of transfer RNA-like molecules synthesized following infection of Escherichia coli by T-even bacteriophages. *J. Biol. Chem.* **253**, 7910–7917
49. Goldfarb, A., and Daniel, V. (1980) Transcriptional control of two gene subclusters in the tRNA operon of bacteriophage T4. *Nature* **286**, 418–420
50. Seidman, J. G., Barrell, B. G., and McClain, W. H. (1975) Five steps in the conversion of a large precursor RNA into bacteriophage proline and serine transfer RNAs. *J. Mol. Biol.* **99**, 733–760
51. Guerrier-Takada, C., McClain, W. H., and Altman, S. (1984) Cleavage of tRNA precursors by the RNA subunit of E. coli ribonuclease P (M1 RNA) is influenced by 3'-proximal CCA in the substrate. *Cell* **34**, 219–224
52. McClain, W. H., Wilson, J. H., and Seidman, J. G. (1988) Genetic analysis of structure and function in phage T4 tRNASer. *J. Mol. Biol.* **203**, 549–553
53. Kazantsev, A. V., and Pace, N. R. (2006) Bacterial RNase P: a new view of an ancient enzyme. *Nat. Rev. Microbiol.* **4**, 729–740
54. Kirsebom, L. A. (2007) RNase P RNA mediated cleavage: substrate recognition and catalysis. *Biochimie* **89**, 1183–1194
55. Lai, L. B., Vioque, A., Kirsebom, L. A., and Gopalan, V. (2010) Unexpected diversity of RNase P, an ancient tRNA processing enzyme: challenges and prospects. *FEBS Lett.* **584**, 287–296
56. Orellana, O., Cooley, L., and Söll, D. (1986) The additional guanylate at the 5' terminus of Escherichia coli tRNAHis is the result of unusual processing by RNase P. *Mol. Cell Biol.* **6**, 525–529
57. Burkard, U., Willis, I., and Söll, D. (1988) Processing of histidine transfer RNA precursors. Abnormal cleavage site for RNase P. *J. Biol. Chem.* **263**, 2447–2451
58. Green, C. J., and Vold, B. S. (1988) Structural requirements for processing of synthetic tRNAHis precursors by the catalytic RNA component of RNase P. *J. Biol. Chem.* **263**, 652–657
59. Reich, C., Olsen, G. J., Pace, B., and Pace, N. R. (1988) Role of the protein moiety of ribonuclease P, a ribonucleoprotein enzyme. *Science* **239**, 178–181
60. Jackman, J. E., Gott, J. M., and Gray, M. W. (2012) Doing it in reverse: 3'-to-5' polymerization by the Thg1 superfamily. *RNA* **18**, 886–899
61. Holm, P. S., and Krupp, G. (1992) The acceptor stem in pre-tRNAs determines the cleavage specificity of RNase P. *Nucleic Acids Res.* **20**, 421–423
62. Kirsebom, L. A., and Svärd, S. G. (1992) The kinetics and specificity of cleavage by RNase P is mainly dependent on the structure of the amino acid acceptor stem. *Nucleic Acids Res.* **20**, 425–432
63. Vold, B. S., and Green, C. J. (1988) Processing of a multimeric tRNA precursor from Bacillus subtilis by the RNA component of RNase P. *J. Biol. Chem.* **263**, 14390–14396
64. McClain, W. H., Guerrier-Takada, C., and Altman, S. (1987) Model substrate for an RNA enzyme. *Science* **238**, 527–530
65. Ladner, J. E., Jack, A., Robertus, J. D., Brown, R. S., Rhodes, D., Clark, B. F. C., *et al.* (1975) Structure of yeast phenylalanine transfer RNA at 2.5 Å resolution. *Proc. Natl. Acad. Sci. U. S. A.* **72**, 4414–4418
66. Quigley, G. J., Wang, A. H., Seeman, N. C., Suddath, F. L., Rich, A., Sussman, J. L., *et al.* (1975) Hydrogen bonding in yeast phenylalanine transfer RNA. *Proc. Natl. Acad. Sci. U. S. A.* **72**, 4866–4870
67. Liu, F., and Altman, S. (1994) Differential evolution of substrates for an RNA enzyme in the presence and absence of its protein cofactor. *Cell* **77**, 1093–1100
68. Pan, T. (1995) Novel RNA substrates for the ribozyme from Bacillus subtilis ribonuclease P identified by *in vitro* selection. *Biochemistry* **34**, 8458–8464
69. Loria, A., and Pan, T. (2000) The 3' substrate determinants for the catalytic efficiency of the Bacillus subtilis RNase P holoenzyme suggest autocatalytic processing of the RNase P RNA *in vivo*. *RNA* **6**, 1413–1422
70. Hansen, A., Pfeiffer, T., Zuleeg, T., Limmer, S., Ciesiolka, J., Feltens, R., *et al.* (2001) Exploring the minimal substrate requirements for trans-cleavage by RNase P holoenzymes from Escherichia coli and Bacillus subtilis. *Mol. Microbiol.* **41**, 131–143
71. Svärd, S. G., and Kirsebom, L. A. (1992) Several regions of a tRNA precursor determine the Escherichia coli RNase P cleavage site. *J. Mol. Biol.* **227**, 1019–1031

72. Perrault, J. P., and Altman, S. (1992) Important 2'-hydroxyl groups in model substrates for M1 RNA, the catalytic RNA subunit of RNase P from Escherichia coli. *J. Mol. Biol.* **226**, 399–409
73. Lundberg, U., and Altman, S. (1995) Processing of the precursor to the catalytic RNA subunit of RNase P from Escherichia coli. *RNA* **1**, 327–334
74. Kim, S., Sim, S., and Lee, Y. (1999) *In vitro* analysis of processing at the 3'-end of precursors of M1 RNA, the catalytic subunit of Escherichia coli RNase P: multiple pathways and steps for the processing. *Nucleic Acids Res.* **27**, 895–902
75. Caruthers, M. H. (2013) The chemical synthesis of DNA/RNA: our gift to science. *J. Biol. Chem.* **288**, 1420–1427
76. Wu, S., Chen, Y., Mao, G., Trobro, S., Kwiatkowski, M., and Kirsebom, L. A. (2014) Transition-state stabilization in Escherichia coli ribonuclease P RNA-mediated cleavage of model substrates. *Nucleic Acids Res.* **42**, 631–642
77. Guerrier-Takada, C., and Altman, S. (1992) Reconstitution of enzymatic activity from fragments of M1 RNA. *Proc. Natl. Acad. Sci. U. S. A.* **89**, 1266–1270
78. Talbot, S. J., and Altman, S. (1994) Gel retardation analysis of the interaction between C5 protein and M1 RNA in the formation of the ribonuclease P holoenzyme from Escherichia coli. *Biochemistry* **33**, 1399–1405
79. Pan, T. (1995) Higher order folding and domain analysis of the ribozyme from Bacillus subtilis ribonuclease P. *Biochemistry* **34**, 902–909
80. Green, C. J., Rivera-León, R., and Vold, B. S. (1996) The catalytic core of RNase P. *Nucleic Acids Res.* **24**, 149–1503
81. Pan, T., and Jakacka, M. (1996) Multiple substrate binding sites in the ribozyme from Bacillus subtilis RNase P. *EMBO J.* **15**, 2249–2255
82. Loria, A., and Pan, T. (1999) The cleavage step of ribonuclease P catalysis is determined by ribozyme-substrate interactions both distal and proximal to the cleavage site. *Biochemistry* **38**, 8612–8620
83. Wu, S., Kikovska, E., Lindell, M., and Kirsebom, L. A. (2012) Cleavage mediated by the catalytic domain of bacterial RNase P RNA. *J. Mol. Biol.* **422**, 204–214
84. Mao, G., Srivastava, A. S., Wu, S., Kosek, D., Lindell, M., and Kirsebom, L. A. (2018) Critical domain interactions for type A RNase P RNA catalysis with and without the specificity domain. *PLoS One* **13**, e0192873
85. Reilly, R. M., and RajBhandary, U. L. (1986) A single mutation in loop IV of Escherichia coli SuIII tRNA blocks processing at both 5'- and 3'-ends of the precursor tRNA. *J. Biol. Chem.* **261**, 2928–2935
86. Baer, M. F., Reilly, R. M., McCorkle, G. M., Hai, T. Y., Altman, S., and RajBhandary, U. L. (1988) The recognition by RNase P of precursor tRNAs. *J. Biol. Chem.* **263**, 2344–2351
87. Kahle, D., Wehmeyer, U., and Krupp, G. (1990) Substrate recognition by RNase P and by the catalytic M1 RNA: identification of possible contact points in pre-tRNAs. *EMBO J.* **9**, 1929–1937
88. Nolan, J. M., Burke, D. H., and Pace, N. R. (1993) Circularly permuted tRNAs as specific photoaffinity probes of ribonuclease P RNA structure. *Science* **261**, 762–765
89. Svärd, S. G., and Kirsebom, L. A. (1993) Determinants of Escherichia coli RNase P cleavage site selection: a detailed *in vitro* and *in vivo* analysis. *Nucleic Acids Res.* **21**, 427–434
90. Gaur, R. K., Hanne, A., Conrad, F., Kahle, D., and Krupp, G. (1996) Differences in the interaction of Escherichia coli RNase P RNA with tRNAs containing a short or a long extra arm. *RNA* **2**, 674–681
91. Loria, A., and Pan, T. (1997) Recognition of the T stem-loop of a pre-tRNA substrate by the ribozyme from Bacillus subtilis ribonuclease P. *Biochemistry* **36**, 6317–6325
92. Loria, A., and Pan, T. (1998) Recognition of the 5' leader and the acceptor stem of a pre-tRNA substrate by the ribozyme from Bacillus subtilis RNase P. *Biochemistry* **37**, 10126–10133
93. Pan, T., Loria, A., and Zhong, K. (1995) Probing of tertiary interactions in RNA: 2'-hydroxyl-base contacts between the RNase P RNA and pre-tRNA. *Proc. Natl. Acad. Sci. U. S. A.* **92**, 12510–12514
94. LaGrandeur, T. E., Hüttenhofer, A., Noller, H. F., and Pace, N. R. (1994) Phylogenetic comparative chemical footprint analysis of the interaction between ribonuclease P RNA and tRNA. *EMBO J.* **13**, 3945–3952
95. Zhang, J., and Ferré-D'Amaré, A. R. (2016) The tRNA elbow in structure, recognition and evolution. *Life* **6**, 3
96. Wu, S., Chen, Y., Lindell, M., Mao, G., and Kirsebom, L. A. (2011) Functional coupling between a distal interaction and the cleavage site in bacterial RNase-P-RNA-mediated cleavage. *J. Mol. Biol.* **411**, 384–396
97. Brännvall, M., and Kirsebom, L. A. (1999) Manganese ions induce miscleavage in the Escherichia coli RNase P RNA-catalyzed reaction. *J. Mol. Biol.* **292**, 53–63
98. Brännvall, M., Kikovska, E., Wu, S., and Kirsebom, L. A. (2007) Evidence for induced fit in bacterial RNase P RNA-mediated cleavage. *J. Mol. Biol.* **372**, 1149–1164
99. Guerrier-Takada, C., Lumelsky, N., and Altman, S. (1989) Specific interactions in RNA enzyme-substrate complexes. *Science* **246**, 1578–1584
100. Heide, C., Busch, S., Feltens, R., and Hartmann, R. K. (2001) Distinct modes of mature and precursor tRNA binding to Escherichia coli RNase P RNA revealed by NAIM analyses. *RNA* **7**, 553–564
101. Pomeranz Krummel, D. A., and Altman, S. (1999) Multiple binding modes of substrate to the catalytic RNA subunit of RNase P from Escherichia coli. *RNA* **5**, 1021–1033
102. Bothwell, A. L., Stark, B. C., and Altman, S. (1976) Ribonuclease P substrate specificity: cleavage of a bacteriophage phi80 induced RNA. *Proc. Natl. Acad. Sci. U. S. A.* **73**, 1912–1916
103. Carrara, G., Calandra, P., Fruscoloni, P., Doria, M., and Tocchini-Valentini, G. P. (1989) Site selection by Xenopus laevis RNAse P. *Cell* **58**, 37–45
104. Thurlow, D. L., Shilowski, D., and Marsh, T. L. (1991) Nucleotides in precursor tRNAs that are required intact for catalysis by RNase P RNAs. *Nucleic Acids Res.* **19**, 885–891
105. Koshland, D. E. (1958) Application of a theory of enzyme specificity to protein synthesis. *Proc. Natl. Acad. Sci. U. S. A.* **44**, 98–104
106. Haas, E. S., Brown, J. W., Pitulle, C., and Pace, N. R. (1994) Further perspective on the catalytic core and secondary structure of ribonuclease P RNA. *Proc. Natl. Acad. Sci. U. S. A.* **91**, 2527–2531
107. Schlegl, J., Hardt, W.-D., Erdmann, V. A., and Hartmann, R. K. (1994) Contribution of structural elements to Thermus thermophilus ribonuclease P RNA function. *EMBO J.* **13**, 4863–4869
108. Pomeranz Krummel, D. A., and Altman, S. (1999) Verification of phylogenetic predictions *in vivo* and the importance of the tetraloop motifif in a catalytic RNA. *Proc. Natl. Acad. Sci. U. S. A.* **96**, 11200–11205
109. Haas, E. S., Morse, D. P., Brown, J. W., Schmidt, F. J., and Pace, N. R. (1991) Long-range structure in ribonuclease P RNA. *Science* **254**, 853–856
110. Marszalkowski, M., Willkomm, D. K., and Hartmann, R. K. (2008) Structural basis of a ribozyme's thermostability: P1-L9 interdomain interaction in RNase P RNA. *RNA* **14**, 127–133
111. Persson, T., Cuzic, S., and Hartmann, R. K. (2003) Catalysis by RNase P RNA: unique features and unprecedented active site plasticity. *J. Biol. Chem.* **278**, 43394–43401
112. Brännvall, M., Kikovska, E., and Kirsebom, L. A. (2004) Cross talk between the +73/294 interaction and the cleavage site in RNase P RNA mediated cleavage. *Nucleic Acids Res.* **32**, 5418–5429
113. Abe, T., Inokuchi, H., Yamada, Y., Muto, A., Iwasaki, Y., and Ikemura, T. (2014) tRNADB-CE: tRNA gene database well-timed in the era of big sequence data. *Front. Genet.* **15**, 114
114. Crothers, D. M., Seno, T., and Söll, D. (1972) Is there a discriminator site in transfer RNA? *Proc. Natl. Acad. Sci. U. S. A.* **69**, 3063–3067
115. Kirsebom, L. A., and Svärd, S. G. (1994) Base pairing between Escherichia coli RNase P RNA and its substrate. *EMBO J.* **13**, 4870–4876
116. Svärd, S. G., Kagardt, U., and Kirsebom, L. A. (1996) Phylogenetic comparative mutational analysis of the base-pairing between RNase P RNA and its substrate. *RNA* **2**, 463–472
117. Oh, B. K., and Pace, N. R. (1994) Interaction of the 3'-end of tRNA with ribonuclease P RNA. *Nucleic Acids Res.* **22**, 4087–4094
118. Busch, S., Kirsebom, L. A., Notbohm, H., and Hartmann, R. K. (2000) Differential role of the intermolecular base-pairs G292-C(75) and G293-C(74) in the reaction catalyzed by Escherichia coli RNase P RNA. *J. Mol. Biol.* **299**, 941–951

119. Wegscheid, B., and Hartmann, R. K. (2007) *In vivo* and *in vitro* investigation of bacterial type B interaction with tRNA 3'-CCA. *Nucleic Acids Res.* **35**, 2060–2073
120. Wegscheid, B., and Hartmann, R. K. (2006) The precursor tRNA 3'-CCA interaction with Escherichia coli RNase P RNA is essential for catalysis *in vivo*. *RNA* **12**, 2135–2148
121. Kikovska, E., Wu, S., Mao, G., and Kirsebom, L. A. (2012) Cleavage mediated by the P15 domain of bacterial RNase P RNA. *Nucleic Acids Res.* **40**, 2224–2233
122. Pyle, A. M. (2016) Group II intron self-splicing. *Annu. Rev. Biophys.* **45**, 183–205
123. Gray, M. W., and Gopalan, V. (2020) Piece by piece: Building a ribozyme. *J. Biol. Chem.* **295**, 2313–2323
124. Ikemura, T., Shimura, Y., Sakano, H., and Ozeki, H. (1975) Precursor molecules of Escherichia coli transfer RNAs accumulated in temperature-sensitive mutant. *J. Mol. Biol.* **96**, 69–86
125. Kole, R., Baer, M. F., Stark, B. C., and Altman, S. (1980) E. coli RNAse P has a required RNA component. *Cell* **19**, 881–887
126. Vioque, A., Arnez, J., and Altman, S. (1988) Protein-RNA interactions in the RNase P holoenzyme from Escherichia coli. *J. Mol. Biol.* **202**, 835–848
127. Rivera-León, R., Green, C. J., and Vold, B. S. (1995) High-level expression of soluble recombinant RNase P protein from Escherichia coli. *J. Bacteriol.* **177**, 2564–2566
128. Niranjanakumari, S., Kurz, J. C., and Fierke, C. A. (1998) Expression, purification and characterization of the recombinant ribonuclease P protein component form Bacillus subtilis. *Nucleic Acids Res.* **26**, 3090–3096
129. Talbot, S. J., and Altman, S. (1994b) Kinetic and thermodynamic analysis of RNA-protein interactions in the RNase P holoenzyme from Escherichia coli. *Biochemistry* **33**, 1406–1411
130. Baer, M. F., Wesolowski, D., and Altman, S. (1989) Characterization *in vitro* of the defect in a temperature-sensitive mutant of the protein subunit of RNase P from Escherichia coli. *J. Bacteriol.* **171**, 6862–6866
131. Gopalan, V., Baxevanis, A. D., Landsman, D., and Altman, S. (1997) Analysis of the functional role of conserved residues in the protein subunit of ribonuclease P from Escherichia coli. *J. Mol. Biol.* **267**, 818–829
132. Biswas, R., Ledman, D. W., Fox, R. O., Altman, S., and Gopalan, V. (2000) Mapping RNA-protein interactions in ribonuclease P from Escherichia coli using disulfide-linked EDTA-Fe. *J. Mol. Biol.* **296**, 19–31
133. Tsai, H.-Y., Masquida, B., Biswas, R., Westhof, E., and Gopalan, V. (2003) Molecular modeling of the three-dimensional structure of the bacterial RNase P holoenzyme. *J. Mol. Biol.* **325**, 661–675
134. Buck, A. H., Kazantsev, A. V., Dalby, A. B., and Pace, N. R. (2005) Structural perspective on the activation of RNase P RNA by protein. *Nat. Struct. Mol. Biol.* **12**, 958–964
135. Lumelsky, N., and Altman, S. (1988) Selection and characterization of randomly produced mutants in the gene coding for M1 RNA. *J. Mol. Biol.* **202**, 443–454
136. Buck, A. H., Dalby, A. B., Poole, A. W., Kazantsev, A. V., and Pace, N. R. (2005) Protein activation of a ribozyme: the role of bacterial RNase P protein. *EMBO J.* **24**, 3360–3368
137. Hsieh, J., Andrews, A. J., and Fierke, C. A. (2004) Roles of protein subunits in RNA-protein complexes: lessons from ribonuclease P. *Biopolymers* **73**, 79–89
138. Sun, L., Campell, F. E., Zahler, N. H., and Harris, M. E. (2006) Evidence that substrate-specific effects of C5 protein lead to uniformity in binding and catalysis by RNase P. *EMBO J.* **25**, 3998–4007
139. Kirsebom, L. A., and Trobro, S. (2009) RNase P RNA-mediated cleavage. *IUBMB Life* **61**, 189–200
140. Kim, Y., and Lee, Y. (2009) Novel function of C5 protein as a metabolic stabilizer of M1 RNA. *FEBS Lett.* **583**, 419–424
141. Henkels, C. H., Kurz, J. C., Fierke, C. A., and Oas, T. G. (2001) Linked folding and anion binding of the Bacillus subtilis ribonuclease P protein. *Biochemistry* **40**, 2777–2789
142. Son, A., Choi, S. I. I., Han, G., and Seong, B. L. (2015) M1 RNA is important for the in-cell solubility of its cognate C5 protein: implications for RNA-mediated protein folding. *RNA Biol.* **12**, 1198–1208
143. Niranjanakumari, S., Stams, T., Crary, S. M., Christianson, D. W., and Fierke, C. A. (1998) Protein component of the ribozyme ribonuclease P alters substrate recognition by directly contacting precursor tRNA. *Proc. Natl. Acad. Sci. U. S. A.* **95**, 15212–15217
144. Spitzfaden, C., Nicholson, N., Jones, J. J., Guth, S., Lehr, R., Prescott, C. D., *et al.* (2000) The structure of ribonuclease P protein from Staphylococcus aureus reveals a unique binding site for single-stranded RNA. *J. Mol. Biol.* **295**, 105–115
145. Jovanovic, M., Sanchez, R., Altman, S., and Gopalan, V. (2002) Elucidation of structure-function relationships in the protein subunit of bacterial RNase P using a genetic complementation approach. *Nucleic Acids Res.* **30**, 5065–5073
146. Kazantsev, A., Krivenko, A. A., Harrington, D. J., Carter, R. J., Holbrook, S. R., Adams, P. D., *et al.* (2003) High-resolution structure of RNase P protein from Thermotoga maritima. *Proc. Natl. Acad. Sci. U. S. A.* **100**, 7497–7502
147. Rueda, D., Hsieh, J., Day-Storms, J. J., Fierke, C. A., and Walter, N. G. (2005) The 5' leader of precursor $tRNA^{Asp}$ bound to the Bacillus subtilis RNase P holoenzyme has an extended conformation. *Biochemistry* **44**, 16130–16139
148. Hsieh, J., Koutmou, K. S., Rueda, D., Koutmos, M., Walter, N. G., and Fierke, C. A. (2010) A divalent cation stabilizes the active conformation of the B. subtilis RNase P•pre-tRNA complex: a role for an inner-sphere metal ion in RNase P. *J. Mol. Biol.* **400**, 38–51
149. Crary, S. M., Niranjanakumari, S., and Fierke, C. A. (1998) The protein component of Bacillus subtilis ribonuclease P increases catalytic efficiency by enhancing interactions with the 5' leader sequence of pre-tRNAAsp. *Biochemistry* **37**, 9409–9416
150. Sun, L., Campell, F. E., Lindsay, E. Y., and Harris, M. E. (2010) Binding of C5 protein to P RNA enhances the rate constant for catalysis for P RNA processing of pre-tRNAs lacking a consensus (+1)/C(+72) pair. *J. Mol. Biol.* **395**, 1019–1037
151. Pettersson, B. M. F., Ardell, D. H., and Kirsebom, L. A. (2005) The length of the 5' leader of Escherichia coli tRNA precursors influences bacterial growth. *J. Mol. Biol.* **351**, 9–15
152. Kurz, J. C., and Fierke, C. A. (2002) The affinity of magnesium binding sites in the Bacillus subtilis RNase P x pre-tRNA complex is enhanced by the protein subunit. *Biochemistry* **41**, 9545–9548
153. Sun, L., and Harris, M. E. (2007) Evidence that binding of C5 protein to P RNA enhances ribozyme catalysis by influencing active site metal ion affinity. *RNA* **13**, 1505–1515
154. Guenther, U.-P., Yandek, L. E., Niland, C. N., Campbell, F. E., Anderson, D., Anderson, V. E., *et al.* (2013) Hidden specificity in an apparently nonspecific RNA-binding protein. *Nature* **502**, 385–388
155. Lin, H. C., Zhao, J., Niland, C. N., Tran, B., Jankowsky, E., and Harris, M. E. (2016) Analysis of the RNA binding specificity landscape of C5 protein reveals structure and sequence preferences that direct RNase P specificity. *Cell Chem. Biol.* **23**, 1271–1281
156. Niland, C. N., Zhao, J., Lin, H.-C., Anderson, D. R., Jankowsky, E., and Harris, M. E. (2016) Determination of the specificity landscape of ribonuclease P processing of precursor tRNA 5' leader sequences. *ACS Chem. Biol.* **11**, 2285–2292
157. Niland, C. N., Anderson, D. R., Jankowsky, E., and Harris, M. E. (2017) The contribution of the C5 protein subunit of Escherichia coli ribonuclease P to specificity for precursor tRNA is modulated by proximal 5' leader sequences. *RNA* **23**, 1502–1511
158. Koutmou, K. S., Zahler, N. H., Kurz, J. C., Campell, F. E., Harris, M. E., and Fierke, C. A. (2010) Protein-precursor tRNA contact leads to sequence-specific recognition of 5' leaders by bacterial ribonuclease P. *J. Mol. Biol.* **396**, 195–208
159. Reiter, N. J., Osterman, A. K., and Mondragón, A. (2012) The bacterial ribonuclease P holoenzyme requires specific, conserved residues for efficient catalysis and substrate positioning. *Nucleic Acids Res.* **40**, 10384–10393
160. Zahler, N. H., Christian, E. L., and Harris, M. E. (2003) Recognition of the 5' leader of pre-tRNA substrates by the active site of ribonuclease P. *RNA* **9**, 734–745

161. Zahler, N. H., Sun, L., Christian, E. L., and Harris, M. E. (2005) The pre-tRNA nucleotide base and 2'-hyrdroxyl at N(-1) contribute to fidelity in tRNA processing by RNase P. *J. Mol. Biol.* **345**, 969–985
162. Behra, P. R. K., Pettersson, B. M. F., Das, S., Dasgupta, S., and Kirsebom, L. A. (2019) Comparative genomics of Mycobacterium mucogenicum and Mycobacterium neoaurum clade members emphasizing tRNA and non-coding RNA. *BMC Evol. Biol.* **19**, 124
163. Brännvall, M., and Kirsebom, L. A. (2005) Complexity in orchestration of chemical groups near different cleavage sites in RNase P RNA mediated cleavage. *J. Mol. Biol.* **351**, 251–257
164. Mao, G., Srivastava, A. S., Wu, S., Kosek, D., and Kirsebom, L. A. (2023) Importance of residue 248 in Escherichia coli RNase P RNA mediated cleavage. *Sci. Rep.* **13**, 14140
165. Siew, D., Zahler, N. H., Cassano, A. G., Strobel, S. A., and Harris, M. E. (1999) Identification of adenosine functional groups involved in substrate binding by the ribonuclease P ribozyme. *Biochemistry* **38**, 1873–1883
166. Burgin, A. B., and Pace, N. R. (1990) Mapping the active site of ribonuclease P RNA using a substrate containing a photoaffinity agent. *EMBO J.* **9**, 4111–4118
167. Harris, M. E., Nolan, J. M., Malhotra, A., Brown, J. W., Harvey, S. C., and Pace, N. R. (1994) Use of photoaffinity crosslinking and molecular modeling to analyze the global architecture of ribonuclease P RNA. *EMBO J.* **13**, 3953–3963
168. Harris, M. E., Kazantsev, A. V., Chen, J. L., and Pace, N. R. (1997) Analysis of the tertiary structure of the ribonuclease P ribozyme-substrate complex by site-specific photoaffinity crosslinking. *RNA* **3**, 561–576
169. Christian, E. L., McPheeters, D. S., and Harris, M. E. (1998) Identification of individual nucleotides in the bacterial ribonuclease P ribozyme adjacent to the pre-tRNA cleavage site by short-range photo-cross-linking. *Biochemistry* **37**, 17618–17628
170. Kirsebom, L. A., and Svärd, S. G. (2000) Ribozyme biochemistry and biotechnology, 2000. In: Krupp, G., Gaur, R. K., eds. *RNase P Processing tRNA Precursors*. Eaton Publishing, Natick, MA: 111–131
171. Svärd, S. G., Mattsson, J. G., Johansson, K. E., and Kirsebom, L. A. (1994) Cloning and characterization of the RNase P RNA genes from two porcine mycoplasmas. *Mol. Microbiol.* **11**, 849–859
172. Brännvall, M., Mattsson, J. G., Svärd, S. G., and Kirsebom, L. A. (1998) RNase P RNA structure and cleavage reflect the primary structure of tRNA genes. *J. Mol. Biol.* **283**, 771–783
173. Meinnel, T., and Blanquet, S. (1995) Maturation of pre-tRNAfMet by Escherichia coli RNase P is specified by a guanosine of the 5'-flanking sequence. *J. Biol. Chem.* **270**, 15908–15914
174. Lazard, M., and Meinnel, T. (1998) Role of base G-2 of pre-tRNAfMet in cleavage site selection by Escherichia coli RNase P *in vitro*. *Biochemistry* **37**, 6041–6049
175. Kazakov, S., and Altman, S. (1991) Site-specific cleavage by metal ion cofactors and inhibitors of M1 RNA, the catalytic subunit of RNase P from Escherichia coli. *Proc. Natl. Acad. Sci. U. S. A.* **88**, 9193–9197
176. Perrault, J. P., and Altman, S. (1993) Pathway of activation by magnesium ions of substrates for the catalytic RNA subunit of RNase P from Escherichia coli. *J. Mol. Biol.* **230**, 750–756
177. Kirsebom, L. A. (2010) Ribonuclease P. protein reviews, Vol 10. In: Liu, F., Altman, S., eds. *Roles of Metal Ions in RNase P Catalysis*, Springer, New York, Dordrecht, Heidelberg, London: 113–134
178. Müller, J. (2010) Functional metal ions in nucleic acids. *Metallomics* **2**, 318–327
179. Auffinger, P., Grover, N., and Westhof, E. (2011) Metal ion binding to RNA. *Met. Ions Life Sci.* **9**, 1–35
180. Pan, T., and Sosnick, T. R. (2006) RNA folding during transcription. *Annu. Rev. Biophys. Biomol. Struct.* **35**, 161–175
181. Baird, N. J., Fang, X.-W., Srividya, N., Pan, T., and Sosnick, T. R. (2007) Folding of a universal ribozyme: the ribonuclease P RNA. *Q. Rev. Biophys.* **40**, 113–161
182. Gardiner, K. J., Marsh, T. L., and Pace, N. R. (1985) Ion dependence of the Bacillus subtilis RNase P reaction. *J. Biol. Chem.* **260**, 5415–5419
183. Guerrier-Takada, C., Haydock, K., Allen, L., and Altman, S. (1986) Metal ion requirements and other aspects of the reaction catalyzed by M1 RNA, the RNA subunit of ribonuclease P from Escherichia coli. *Biochemistry* **25**, 1509–1515
184. Feig, A. L., and Uhlenbeck, O. C. (1999) RNA World II. In: Gesteland, R., Cech, T., Atkins, J., eds. *The Role of Metal Ions in RNA Biochemistry*, Cold Spring Harbor Laboratory Press, Cold Spring Harbor, NY: 287–319
185. Tallsjö, A., Svärd, S. G., Kufel, J., and Kirsebom, L. A. (1993) A novel tertiary interaction in M1 RNA, the catalytic subunit of Escherichia coli RNase P. *Nucleic Acids Res.* **21**, 3927–3933
186. Zito, K., Hüttenhofer, A., and Pace, N. R. (1993) Lead-catalyzed cleavage of ribonuclease P RNA as a probe for integrity of tertiary structure. *Nucleic Acids Res.* **21**, 5916–5920
187. Ciesiolka, J., Hardt, W. D., Schlegl, J., Erdmann, V. A., and Hartmann, R. K. (1994) Lead-ion-induced cleavage of RNase P RNA. *Eur. J. Biochem.* **219**, 49–56
188. Kikovska, E., Brännvall, M., Kufel, J., and Kirsebom, L. A. (2005) Substrate discrimination in RNase P RNA-mediated cleavage: importance of the structural environment of the RNase P cleavage site. *Nucleic Acids Res.* **33**, 2012–2021
189. Kikovska, E., Brännvall, M., and Kirsebom, L. A. (2006) The exocyclic amine at the RNaseP cleavage site contributes to substrate binding and catalysis. *J. Mol. Biol.* **359**, 572–584
190. Forster, A. C., and Altman, S. (1990) External guide sequences for an RNA enzyme. *Science* **249**, 783–786
191. Smith, D., and Pace, N. R. (1993) Multiple magnesium ions in the ribonuclease P reaction mechanism. *Biochemistry* **32**, 6273–6281
192. Warnecke, J. M., Fürste, J. P., Hardt, W. D., Erdmann, V. A., and Hartmann, R. K. (1996) Ribonuclease P (RNase P) RNA is converted to a Cd(2+)-ribozyme by a single Rp-phosphorothioate modification in the precursor tRNA at the RNase P cleavage site. *Proc. Natl. Acad. Sci. U. S. A.* **93**, 8924–8928
193. Chen, Y., Li, X., and Gegenheimer, P. (1997) Ribonuclease P catalysis requires Mg2+ coordinated to the pro-Rp oxygen of the scissile bond. *Biochemistry* **36**, 2425–2438
194. Warnecke, J. M., Held, R., Busch, S., and Hartmann, R. K. (1999) Role of metal ions in the hydrolysis reaction catalyzed by RNase P RNA from Bacillus subtilis. *J. Mol. Biol.* **290**, 433–445
195. Christian, E. L., Smith, K. M., Perera, N., and Harris, M. E. (2006) The P4 metal binding site in RNase P RNA affects active site metal affinity through substrate positioning. *RNA* **12**, 1463–1467
196. Chang, S. E., and Smith, J. D. (1973) Structural studies on a tyrosine tRNA precursor. *Nat. New Biol.* **246**, 165–168
197. McClain, W. H., and Seidman, J. G. (1974) Genetic perturbations that reveal tertiary conformation of tRNA precursor molecules. *Nature* **257**, 106–110
198. Saenger, W. (1984). In *Principles of Nucleic Acid Structure*, Springer, Verlag, New York, Berlin, Heidelberg, Tokyo
199. Steitz, T. A., and Steitz, J. A. (1993) A general two-metal-ion mechanism for catalytic RNA. *Proc. Natl. Acad. Sci. U. S. A.* **90**, 6498–6502
200. Christian, E. L., Kaye, N. M., and Harris, M. E. (2002) Evidence for a polynuclear metal ion binding site in the catalytic binding site in the catalytic core of the ribonuclease P ribozyme. *EMBO J.* **21**, 2253–2262
201. Liu, X., Chen, Y., and Fierke, C. A. (2017) Inner-sphere coordination of divalent metal ion with nucleobase in catalytic RNA. *J. Am. Chem. Soc.* **139**, 17457–17463
202. Vold, B. S. (1985) Structure and organization of genes for transfer ribonucleic acid in Bacillus subtilis. *Microbiol. Rev.* **49**, 71–80
203. Green, C. J. (1995) Transfer RNA gene organization and RNase P. *Mol. Biol. Rep.* **22**, 181–185
204. Bechhofer, D. H., and Deutscher, M. P. (2019) Bacterial ribonucleases and their roles in RNA metabolism. *Crit. Rev. Biochem. Mol. Biol.* **54**, 242–300
205. Mohanty, B. K., and Kushner, S. R. (2019) New insights into the relationship between tRNA processing and polyadenylation in Escherichia coli. *Trends Genet.* **35**, 434–445
206. Söderbom, F., Svärd, S. G., and Kirsebom, L. A. (2005) RNase E cleavage in the 5' leader of a tRNA precursor. *J. Mol. Biol.* **352**, 22–27
207. Fournier, M. J., and Ozeki, H. (1985) Structure and organization of transfer ribonucleic acid genes of Escherichia coli K-12. *Microbiol. Rev.* **49**, 379–397

208. Blattner, F. R., Plunkett, G., 3rd, Bloch, C. A., Perna, N. T., Burland, V., Riley, M., *et al.* (1997) The complete genome sequence of Escherichia coli K-12. *Science* **277**, 1453–1462
209. Schmidt, F. J., Seidman, J. G., and Bock, R. M. (1976) Transfer ribonucleic acid biosynthesis. *J. Biol. Chem.* **251**, 2440–2445
210. Kurz, J. C., Niranjanakumari, S., and Fierke, C. A. (1998) Protein component of Bacillus subtilis RNase P specifically enhances the affinity for precursor-tRNAAsp. *Biochemistry* **37**, 2393–2400
211. Agrawal, A., Mohanty, B. K., and Kushner, S. R. (2014) Processing of the seven valine tRNAs in Escherichia coli involves novel features of RNase P. *Nucleic Acids Res.* **42**, 11166–11179
212. Mohanty, K., and Kushner, S. R. (2007) Ribonuclease P processes polycistronic tRNA transcripts in Escherichia coli independent of ribonuclease E. *Nucleic Acids Res.* **35**, 7614–7625
213. Nomura, T., and Ishihama, A. (1988) A novel function of RNase P from Escherichia coli: processing of a suppressor tRNA precursor. *EMBO J.* **7**, 3539–3545
214. Zhao, J., and Harris, M. E. (2019) Distributive enzyme binding controlled by local RNA context results in 3' to 5' directional processing of dicistronic tRNA precursors by Escherichia coli ribonuclease P. *Nucleic Acids Res.* **47**, 1451–1467
215. Fang, X. W., Yang, X. J., Littrell, K., Niranjanakumari, S., Thiyagarajan, P., Fierke, C. A., *et al.* (2001) The Bacillus subtilis RNase P holoenzyme contains two RNase P RNA and two RNase P protein subunits. *RNA* **7**, 233–241
216. Phan, H.-D., Norris, A. S., Du, C., Stachowski, K., Khairunisa, B. H., Sidharthan, V., *et al.* (2022) Elucidation of structure-function relationships in Methanocaldococcus jannaschii RNase P, a multi-subunit catalytic ribonucleoprotein. *Nucl. Acids Res.* **50**, 8154–8167
217. Bothwell, A. L., Garber, R. L., and Altman, S. (1976) Nucleotide sequence and *in vitro* processing of a precursor molecule to Escherichia coli 4.5 S RNA. *J. Biol. Chem.* **251**, 7709–7716
218. Guerrier-Takada, C., van Belkum, A., Pleij, C. W., and Altman, S. (1988) Novel reactions of RNAse P with a tRNA-like structure in turnip yellow mosaic virus RNA. *Cell* **53**, 267–272
219. Green, C. J., Vold, B. S., Morch, M. D., Joshi, R. L., and Haenni, A. L. (1988) Ionic conditions for the cleavage of the tRNA-like structure of turnip yellow mosaic virus by the catalytic RNA of RNase P. *J. Biol. Chem.* **263**, 11617–11620
220. Alifano, P., Rivellini, F., Piscitelli, C., Arraiano, C. M., Bruni, C. B., and Carlomagno, M. S. (1994) Ribonuclease E provides substrates for ribonuclease P-dependent processing of a polycistronic mRNA. *Genes Dev.* **8**, 3021–3031
221. Komine, Y., Kitabatake, M., Yokogawa, T., Nishikawa, K., and Inokuchi, H. (1994) A tRNA-like structure is present in 10Sa RNA, a small stable RNA from Escherichia coli. *Proc. Natl. Acad. Sci. U. S. A.* **91**, 9223–9227
222. Hartmann, R. K., Heinrich, J., Schlegl, J., and Schuster, H. (1995) Precursor of C4 antisense RNA of bacteriophages P1 and P7 is a substrate for RNase P of Escherichia coli. *Proc. Natl. Acad. Sci. U. S. A.* **92**, 5822–5826
223. Li, Y., and Altman, S. (2003) A specific endoribonuclease, RNase P, affecs gene expression of polycistronic operon mRNAs. *Proc. Natl. Acad. Sci. U. S. A.* **100**, 13213–13218
224. Altman, S., Wesolowski, D., and Guerrier-Takada, C. (2005) RNase P cleaves transient structures in some riboswitches. *Proc. Natl. Acad. Sci. U. S. A.* **102**, 11284–11289
225. Mohanty, B. K., and Kushner, S. R. (2021) Inactivation of RNase P in Escherichia coli significantly changes post-transcriptional RNA metabolism. *Mol. Microbiol.* **117**, 121–142
226. Mohanty, B. K., and Kushner, S. R. (2022) Regulation of mRNA decay in E. coli. *Crit. Rev. Biochem. Mol. Biol.* **57**, 48–72
227. Mans, R. M., Guerrier-Takada, C., Altman, S., and Pleij, C. W. (1990) Interaction of RNase P from Escherichia coli with pseudoknotted structures in viral RNAs. *Nucleic Acids Res.* **18**, 3479–3487
228. Barrera, A., and Pan, T. (2004) Interaction of the Bacillus subtilis RNase P with the 30S ribosomal subunit. *RNA* **10**, 482–492
229. Daoud, R., Forget, L., and Lang, B. F. (2012) Yeast mitochondrial RNase P, RNase Z and the RNA degradosome are part of a stable supercomplex. *Nucleic Acids Res.* **40**, 1728–1736
230. Carpousis, A. J., Campo, N., Hadjeras, L., and Hamouche, L. (2022) Compartmentalization of RNA degradosomes in bacteria controls accessibility to substrates and ensures concerted degradation of mRNA to nucleotides. *Annu. Rev. Microbiol.* **76**, 533–552
231. Yuan, Y., Hwang, E. S., and Altman, S. (1992) Targeted cleavage of mRNA by human RNase P. *Proc. Natl. Acad. Sci. U. S. A.* **89**, 8006–8010
232. Yuan, Y., and Altman, S. (1994) Selection of guide sequences that direct efficient cleavage of mRNA by human ribonuclease P. *Science* **263**, 1269–1273
233. Werner, M., Rosa, E., Nordstrom, J. L., Goldberg, A. R., and George, S. T. (1998) Short oligonucleotides as external guide sequences for site-specific cleavage of RNA molecules with human RNase P. *RNA* **4**, 847–855
234. Liu, F., and Altman, S. (1995) Inhibition of viral gene expression by the catalytic RNA subunit of RNase P from *Escherichia coli*. *Genes Dev.* **9**, 471–480
235. Kim, K., and Liu, F. (2007) Inhibition of gene expression in human cells using RNase P-derived ribozymes and external guide sequences. *Biochim. Biophys. Acta* **1769**, 603–612
236. Guerrier-Takada, C., Li, Y., and Altman, S. (1995) Artificial regulation of gene expression in *Escherichia coli* by RNase P. *Proc. Natl. Acad. Sci. U. S. A.* **92**, 11115–11119
237. Frank, D. N., Harris, M., and Pace, N. R. (1994) Rational design of self-cleaving pre-tRNA-ribonuclease P RNA conjugates. *Biochemistry* **33**, 10800–10808
238. Stein, C. A., and Cheng, Y. C. (1993) Antisense oligonucleotides as therapeutic agents–is the bullet really magical? *Science* **261**, 1004–1012
239. Sarver, N., Cantin, E. M., Chang, P. S., Zaia, J. A., Ladne, P. A., Stephens, D. A., *et al.* (1990) Ribozymes as potential anti-HIV-1 therapeutic agents. *Science* **247**, 1222–1225
240. Sullenger, B. A., and Cech, T. R. (1994) Ribozyme-mediated repair of defective mRNA by targeted, trans-splicing. *Nature* **371**, 619–622
241. Yu, M., Ojwang, J., Yamada, O., Hampel, A., Rapapport, J., Looney, D., *et al.* (1993) A hairpin ribozyme inhibits expression of diverse strains of human immunodeficiency virus type 1. *Proc. Natl. Acad. Sci. U. S. A.* **90**, 6340–6344
242. Ranasinghe, P., Addison, M. L., Dear, J. W., and Webb, D. J. (2023) Small interfering RNA: discovery, pharmacology and clinical development-An introductory review. *Br. J. Pharmacol.* **180**, 2697–2720
243. Wang, J. Y., and Doudna, J. A. (2023) CRISPR technology: a decade of genome editing is only the beginning. *Science* **379**, eadd8643
244. Sparmann, A., and Vogel, J. (2023) RNA-based medicine: from molecular mechanisms to therapy. *EMBO J.* **42**, e114760
245. Altman, S. (2014) Antibiotics present and future. *FEBS Lett.* **588**, 1–2
246. Garg, A., Wesolowski, D., Alonso, D., Deitsch, K. W., Ben Mamoun, C., and Altman, S. (2015) Targeting protein translation, RNA splicing, and degradation by morpholino-based conjugates in Plasmodium falciparum. *Proc. Natl. Acad. Sci. U. S. A.* **112**, 11935–11940
247. Yan, B., Liu, Y., Chen, Y. C., and Liu, F. (2023) A RNase P ribozyme inhibits gene expression and replication of hepatitis B virus in cultured cells. *Microorganisms* **11**, 654
248. Liu, Y., Chen, Y. C., Yan, B., and Liu, F. (2023) Suppressing Kaposi's sarcoma-associated herpesvirus lytic gene expression and replication by RNase P ribozyme. *Molecules* **28**, 3619
249. Plehn-Dujowich, D., and Altman, S. (1998) Effective inhibition of influenza virus production in cultured cells by external guide sequences and ribonuclease P. *Proc. Natl. Acad. Sci. U. S. A.* **95**, 7327–7332
250. Trang, P., Lee, M., Nepomuceno, E., Kim, J., Zhu, H., and Liu, F. (2000) Effective inhibition of human cytomegalovirus gene expression and replication by a ribozyme derived from the catalytic RNA subunit of RNase P from Escherichia coli. *Proc. Natl. Acad. Sci. U. S. A.* **97**, 5812–5817
251. Zou, H., Lee, J., Kilani, A. F., Kim, K., Trang, P., Kim, J., *et al.* (2004) Engineered RNase P ribozymes increase their cleavage activities and efficacies in inhibiting viral gene expression in cells by enhancing the rate of cleavage and binding of the target mRNA. *J. Biol. Chem.* **279**, 32063–32070
252. Zhu, J., Trang, P., Kim, K., Zhou, T., Deng, H., and Liu, F. (2004) Effective inhibition of Rta expression and lytic replication of Kaposi's

sarcoma-associated herpesvirus by human RNase P. *Proc. Natl. Acad. Sci. U. S. A.* **101**, 9073–9078
253. Bai, Y., Trang, P., Li, H., Kim, K., Zhou, T., and Liu, F. (2008) Effective inhibition in animals of viral pathogenesis by a ribozyme derived from RNase P catalytic RNA. *Proc. Natl. Acad. Sci. U. S. A.* **105**, 10919–10924
254. Xia, C., Chen, Y. C., Gong, H., Zeng, W., Vu, G. P., Trang, P., *et al.* (2013) Inhibition of hepatitis B virus gene expression and replication by ribonuclease P. *Mol. Ther.* **21**, 995–1003
255. Kilani, A. F., Trang, P., Jo, S., Hsu, A., Kim, J., Nepomuceno, E., *et al.* (2000) RNase P ribozymes selected *in vitro* to cleave a viral mRNA effectively inhibit its expressionin cell culture. *J. Biol. Chem.* **275**, 10611–10622
256. Liu, F., ed. (2010) *Ribonuclease P as a Tool*. Springer, New York
257. Li, W., Liu, Y., Wang, Y., Li, R., Trang, P., Tang, W., *et al.* (2018) Engineered RNase P ribozymes effectively inhibit the infection of murine cytomegalovirus in animals. *Theranostics* **8**, 5634–5644
258. Li, W., Sheng, J., Xu, M., Vu, G. P., Yang, Z., Liu, Y., *et al.* (2017) Inhibition of murine cytomegalovirus infection in animals by RNase P-associated external guide sequences. *Mol. Ther. Nucleic Acids* **9**, 322–332
259. Raj, S. M., and Liu, F. (2003) Engineering of RNase P ribozyme for gene-targeting applications. *Gene* **313**, 59–69
260. Sun, X., Chen, W., He, L., Sheng, J., Liu, Y., Vu, G. P., *et al.* (2017) Inhibition of human cytomegalovirus immediate early gene expression and growth by a novel RNase P ribozyme variant. *PLoS One* **12**, e0186791
261. Trang, P., Hsu, A., Zhou, T., Lee, J., Kilani, A. F., Nepomuceno, E., *et al.* (2002) Engineered RNase P ribozymes inhibit gene expression and growth of cytomegalovirus by increasing rate of cleavage and substrate binding. *J. Mol. Biol.* **315**, 573–586
262. Zhang, Z., Vu, G. P., Gong, H., Xia, C., Chen, Y. C., Liu, F., *et al.* (2013) Engineered external guide sequences are highly effective in inhibiting gene expression and replication of hepatitis B virus in cultured cells. *PLoS One* **8**, e65268
263. Cobaleda, C., and Sanchez-Garcia, I. (2000) *In vitro* inhibition by a site-specific catalytic RNA subunit of RNase P designed against the BCR-ABL oncogenic products: a novel approach for cancer treatment. *Blood* **95**, 731–737
264. Ma, M., Benimetskaya, L., Lebedeva, I., Dignam, J., Takle, G., and Stein, C. A. (2000) Intracellular mRNA cleavage induced through activation of RNase P by nuclease-resistant external guide sequences. *Nat. Biotechnol.* **18**, 58–61
265. McKinney, J. S., Zhang, H., Kubori, T., Galan, J. E., and Altman, S. (2004) Disruption of type III secretion in Salmonella enterica serovar Typhimurium by external guide sequences. *Nucleic Acids Res.* **32**, 848–854
266. Bai, Y., Gong, H., Li, H., Vu, G., Lu, S., and Liu, F. (2011) Oral delivery of RNase P ribozymes by Salmonella inhibits viral infection in mice. *Proc. Natl. Acad. Sci. U. S. A.* **108**, 3222–3227
267. Gibbons, D. L., Shashikant, C., and Hayday, A. C. (2004) A comparative analysis of RNA targeting strategies in the thymosin beta 4 gene. *J. Mol. Biol.* **342**, 1069–1076
268. DiGiusto, D. L., Krishnan, A., Li, L., Li, H., Li, S., Rao, A., *et al.* (2010) RNA-based gene therapy for HIV with lentiviral vector-modified CD34(+) cells in patients undergoing transplantation for AIDS-related lymphoma. *Sci. Transl. Med.* **3**, 36ra43
269. Furdon, P. J., Guerrier-Takada, C., and Altman, S. (1983) A G43 to U43 mutation in E. coli tRNAtyrsu3+ which affects processing by RNase P. *Nucl. Acids Res.* **11**, 1491–1505
270. Steinberg, S., Misch, A., and Sprinzl, M. (1993) Compilation of tRNA sequences and sequences of tRNA genes. *Nucleic Acids Res.* **21**, 3011–3015
271. Massire, C., Jaeger, L., and Westhof, E. (1998) Derivation of the three-dimensional architecture of bacterial ribonuclease P RNAs from comparative sequence analysis. *J. Mol. Biol.* **279**, 773–793
272. Brown, J. (1999) The ribonuclease P database. *Nucleic Acids Res.* **27**, 314
273. Shi, H., and Moore, P. B. (2000) The crystal structure pf yeast phenylalanine tRNA at 1.93 Å resolution: a classic structure revisited. *RNA* **6**, 1091–1105
274. Hnatyszyn, H., Spruill, G., Young, A., Seivright, R., and Kraus, G. (2001) Long-term RNase P-mediated inhibition of HIV-1 replication and pathogenesis. *Gene Ther.* **8**, 1863–1871
275. Kraus, G., Geffin, R., Spruill, G., Young, A. K., Seivright, R., Cardona, D., *et al.* (2002) Cross-clade inhibition of HIV-1 replication and cytopathology by using RNase P-associated external guide sequences. *Proc. Natl. Acad. Sci. U. S. A.* **99**, 3406–3411
276. Bai, Y., Li, H., Vu, G., Gong, H., Umamoto, S., Zhou, T., *et al.* (2010) *Salmonella*-mediated delivery of RNase P ribozymes for inhibition of viral gene expression and replication in human cells. *Proc. Natl. Acad. Sci. U. S. A.* **107**, 7269–7274
277. Deng, Q., Liu, Y., Li, X., Yan, B., Sun, X., Tang, W., *et al.* (2019) Inhibition of human cytomegalovirus major capsid protein expression and replication by ribonuclease P-associated external guide sequences. *RNA* **25**, 645–655
278. Jiang, X., Bai, Y., Rider, P., Kim, K., Zhang, C., Lu, S., *et al.* (2011) Engineered external guide sequences effectively block viral gene expression and replication in cultured cells. *J. Biol. Chem.* **286**, 322–330
279. Liu, J., Shao, L., Trang, P., Yang, Z., Reeves, M., Sun, X., *et al.* (2016) Inhibition of herpes simplex virus 1 gene expression and replication by RNase P-associated external guide sequences. *Sci. Rep.* **6**, 27068
280. Jiang, X., Gong, H., Chen, Y. C., Vu, G. P., Trang, P., Zhang, C. Y., *et al.* (2012) Effective inhibition of cytomegalovirus infection by external guide sequences in mice. *Proc. Natl. Acad. Sci. U. S. A.* **109**, 13070–13075
281. McKinney, J., Guerrier-Takada, C., Wesolowski, D., and Altman, S. (2001) Inhibition of Escherichia coli viability by external guide sequences complementary to two essential genes. *Proc. Natl. Acad. Sci. U. S. A.* **98**, 6605–6610
282. Wesolowski, D., Alonso, D., and Altman, S. (2013) Combined effect of a peptide-morpholino oligonucleotide conjugate and a cell-penetrating peptide as an antibiotic. *Proc. Natl. Acad. Sci. U. S. A.* **110**, 8686–8689
283. Shen, N., Ko, J. H., Xiao, G., Wesolowski, D., Shan, G., Geller, B., *et al.* (2009) Inactivation of expression of several genes in a variety of bacterial species by EGS technology. *Proc. Natl. Acad. Sci. U. S. A.* **106**, 8163–8168
284. Wesolowski, D., Tae, H. S., Gandotra, N., Llopis, P., Shen, N., and Altman, S. (2011) Basic peptide-morpholino oligomer conjugate that is very effective in killing bacteria by gene-specific and nonspecific modes. *Proc. Natl. Acad. Sci. U. S. A.* **108**, 16582–16587
285. Sawyer, A. J., Wesolowski, D., Gandotra, N., Stojadinovic, A., Izadjoo, M., Altman, S., *et al.* (2013) A peptide-morpholino oligomer conjugate targeting Staphylococcus aureus gyrA mRNA improves healing in an infected mouse cutaneous wound model. *Int. J. Pharm.* **453**, 651–655
286. Augagneur, Y., Wesolowski, D., Tae, H. S., Altman, S., and Ben Mamoun, C. (2012) Gene selective mRNA cleavage inhibits the development of Plasmodium falciparum. *Proc. Natl. Acad. Sci. U. S. A.* **109**, 6235–6240
287. Yan, B., Liu, Y., Chen, Y. C., Zhang, I., and Liu, F. (2023) RNase P ribozyme effectively inhibits human CC-chemokine receptor 5 expression and human immunodeficiency virus 1 infection. *Zoonotic Dis.* **3**, 93–103
288. Zeng, W., Vu, G. P., Bai, Y., Chen, Y. C., Trang, P., Lu, S., *et al.* (2013) RNase P-associated external guide sequence effectively reduces the expression of human CC-chemokine receptor 5 and inhibits the infection of human immunodeficiency virus 1. *Biomed. Res. Int.* **2013**, 509714